



**ASHESI UNIVERSITY**

**DESIGN AND CONSTRUCTION OF WATER FILTRATION SYSTEM FOR  
GHANAIAN HOUSEHOLDS**

**CAPSTONE PROJECT**

B.Sc. Mechanical Engineering

**Vera Bordah  
(ID: 27242022)**

**Khadijatu Nayi Alhassan  
(ID: 73692022)**

**Kwame Konadu Boadi  
(ID: 81242022)**

**May 2022**

**ASHESI UNIVERSITY**

**DESIGN AND CONSTRUCTION OF WATER FILTRATION SYSTEM FOR  
GHANAIAN HOUSEHOLDS**

**CAPSTONE PROJECT**

Capstone project submitted to the Department of Engineering, Ashesi University in partial fulfilment of the requirement for the award of Bachelor of Science degree in Mechanical Engineering

**Vera Bordah  
(ID: 27242022)**

**Khadijatu Nayi Alhassan  
(ID: 73692022)**

**Kwame Konadu Boadi  
(ID: 81242022)**

**2022**

## Declarations

We hereby declare that this capstone is the result of my original work and that no part of it has been presented for another degree at this university or elsewhere.

Candidates' Signatures:

Candidates' Names: Vera Bordah    Khadijatu Nayi Alhassan    Kwame Konadu Boadi

Date: 13<sup>th</sup> May 2022.

I hereby declare that the preparation and presentation of this capstone were supervised by the guidelines on the supervision of capstone laid down by Ashesi University.

Supervisor's Signature:

.....

Supervisor's Name:

.....

Date:

.....

## **Acknowledgements**

We start with the name of Allah or God, the most beneficent, the most merciful. We are grateful to the almighty for granting us the strength and sustenance, whose mercy covered every mistake, and whose favour helped us complete this project. Our heartfelt gratitude goes to Ashesi University and the MasterCard Foundation Scholars Program (MCFSP) for allowing us to experience a university education.

Next, we are grateful to Dr. Danyuo Yiporo for his immense contribution to the success of this project in the form of his numerous and invaluable instructions, constructive feedback, and recommendations throughout this project. Thank you very much, Sir. We also thank the Mechanical Engineering lecturers for their input during our presentations. Dr. Elena Rosca, Dr. Stephen Kofi Armah, Miriam Abade-Abugre, and Dr. Heather Beem. Thank you all for the feedback, your input has shaped this project.

We appreciate Mr. Peter Lawerh Kwao and Robert Boateng-Duah for their assistance with fabrication and mechanical testing, respectively. Thank you.

We also appreciate the engineering department for the impactful knowledge, practical experience, necessary equipment, and financial support, which enabled us to complete this project.

## Abstract

Activities of illegal mining and improper waste disposal have mainly contaminated water bodies in Ghana with dirt, heavy metals, and other toxins, making it difficult for communities to acquire safe drinking water. The situation in rural areas aggravates due to the lack of decentralized water supply systems. Poor quality drinking water has numerous health complications and is more severe in children under five. In response to the challenge, a water filtration system was designed and modelled with SolidWorks software. A scaffold was built with extruded aluminium and covered with transparent Perspex glass before part assembling. Grey clay was obtained from the Savannah Region in Ghana for moulding a ceramic filtration unit for dirt and particulate removal. Activated carbon was obtained from coconut coir fibres fired at 900 for 30 mins for particulate and heavy metal adsorption. Other agricultural wastes produced from orange and banana peels were primarily used for heavy metal adsorption. Porous poly-dimethyl-siloxane (PDMS) membrane was obtained via solvent casting and leaching techniques to support the blockage of leaked particles from travelling through the filtration track. Experimental optimizations were done to reduce the turbidity and heavy metal levels in polluted waters. The filtration system proved to be effective in removing zinc, cadmium, copper and suspended particulates from contaminated water samples (compared with WHO recommended limits). Other water quality parameters: pH, conductivity, and turbidity, were regularly used to ascertain filter duration. The flow rates were determined and compared with the WHO limits. The result and implications were discussed to optimise a multipurpose water filtration system for affected communities.

**Keywords:** Ceramic filter, particulate adsorption, heavy metal removal, porous PDMS membrane, orange peels, and activated carbon.

## Table of Content

Declarations .....	ii
Abstract.....	iv
List of Figures.....	ix
List of Tables .....	xii
CHAPTER ONE.....	1
1.0 Introduction.....	1
1.1 Background .....	1
1.2 Demand for Quality Water.....	2
1.3 Problem Statement .....	2
1.4 Motivation.....	3
1.5 Goals and Specific Objectives.....	4
CHAPTER TWO .....	6
2.0 Literature Review.....	6
2.1 Water Contamination .....	6
2.1.1 Inorganic Contaminants.....	6
2.1.2 Heavy Metals and Effects on Human Health .....	7
2.1.3 Organic Contaminants .....	8
2.1.4 Biological Contaminants .....	8
2.1.5 Radiological Contaminants.....	9
2.2 Water Treatment Techniques .....	9
2.2.1 Reverse Osmosis.....	10
2.2.2 Activated Carbon Adsorption.....	11
2.2.3 Solar Water Disinfection .....	11
2.2.4 Ceramic Filter Technique .....	12
2.3 Description of the Poly-dimethyl-siloxane .....	14
2.4 Flow Properties .....	15
2.4.1 Porosity.....	15
2.4.2 Flow rate and Turbidity .....	16
2.4.3 Permeability and Tortuosity .....	16

2.5 Microbial and Virus Removal .....	17
2.5.1 Microbial Removal .....	17
2.5.2 Virus Removal .....	18
2.6 Mechanical Properties .....	19
2.6.1 Elasticity .....	19
2.6.2 Stress and Strain .....	19
2.6.3 Composite Design.....	20
2.7 Scope of Work.....	22
CHAPTER THREE .....	23
3.0 Materials and Methods.....	23
3.1 List of Materials .....	23
3.2 Ceramic Filter Materials.....	24
3.2.1 Clay.....	24
3.2.2 Burnout Material.....	24
3.2.3 Traditional Herbs .....	25
3.3 Requirements of the Filtration system .....	25
3.3.1 Design Requirements.....	25
3.3.2 Functional Requirements.....	26
3.4 Preparation of Ceramic Filter.....	27
3.4.1 Ratio and Mixing .....	27
3.4.2 Soft Working .....	27
3.4.3 Compaction.....	28
3.4.4 Drying and Firing .....	29
3.4.5 Traditional Quenchant Preparation.....	29
3.5 Preparation of PDMS Filter Membranes.....	30
3.5.1 Curing of PDMS samples.....	30
3.5.2 Preparation of PDMS Membrane .....	31
3.5.3 Fabrication of Filter Container .....	32
3.6 Agricultural waste and activated carbon filter .....	33
3.6.1 Preparation of Orange and Banana Peels for Heavy Metal Removal.....	33
3.6.2 Preparation of Activated Carbon .....	34
3.6.3 Activated Carbon and Agricultural Waste Filter Fabrication.....	35

3.7 Selection, Sizing and Justification of Subcomponents.....	36
3.7.1 Ceramic Water Filter .....	36
3.7.2 Submersible Pump and Sizing.....	37
3.8 Design Consideration for Combined Filtration System .....	37
3.9 Operational Mechanism of the Combined System Works .....	38
3.10 The Metallic and Support Structure .....	41
3.10 Optimisations .....	41
3.10.1 Ceramic Filter Impregnation with Colloidal Silver.....	41
3.10.2 Heavy Metal Adsorption .....	42
3.11 Flexural and Compressive Test on Ceramic Composites.....	43
3.12 Tensile Testing of PDMS Specimens.....	45
3.13 Porosity and Density .....	46
3.14 Method of Determining Porosity and Density .....	47
CHAPTER FOUR.....	48
4.0 Results and Analysis.....	48
4.1 Mechanical analysis of the Structural Scaffold.....	48
4.2 Preliminary Water Quality Analysis .....	49
4.2.1 Measuring Flow Rate of Activated and Agricultural Waste Filter.....	49
4.1.2 Water Quality Analysis with a Commercial Granular Activated Carbon .....	51
4.2 Testing the Effectiveness of the Locally Made Activated Carbon.....	53
4.3 Apparent Porosity and Density of Porous Clay Filters .....	54
4.4 Results from Filtration with Ceramic Water Filter .....	55
4.5 FTIR Analysis of the Herbs .....	56
4.6 X-Ray Fluorescence (XRF) Analysis of the Quenchant.....	57
4.7 Tensile Strength of PDMS Samples.....	57
4.7.1 Statistical analysis.....	58
4.8 Effect of thickness of PDMS Filter.....	59
4.8.1 Flow Rate.....	59
4.7.2 Water Quality Analysis using PDMS Filter Membrane.....	60



4.8 Flow Rate of the PDMS Filter.....	61
4.9 Water Quality Analysis of Final Filtrate.....	63
4.9.1 pH, Turbidity and Conductivity Analysis.....	63
4.9.2 Heavy Metal Concentration Analysis.....	64
CHAPTER FIVE .....	65
5.0 Conclusions and Recommendations .....	65
5.1 Conclusions .....	65
5.2 Limitations .....	66
5.3 Recommendations and/or Future Works.....	67
References.....	69
Appendices.....	79
Appendix A: Water Analysis Tests.....	79
Appendix B: Procedure for making Male and Female Mould for Ceramic Water Filter and for determining Density and Porosity.....	81
Appendix C: Pump Sizing Calculations.....	84
Appendix D: Proposed Designs .....	85
.....	85
Appendix E: Steel Structure Analytical Calculations .....	87
Appendix F: Fabrication.....	88
Appendix G: Stress stain graphs obtained from Origin .....	89
Appendix H: Water quality analysis equipment .....	90
Appendix I: Statistical analysis for PDMS membrane.....	91
Appendix J: FTIR and XRF: Laboratory test and Analysis.....	92
Appendix K: Properties of Clay-Sawdust Samples and Water Quality Analysis.....	97

## List of Figures

<b>Figure 2.1:</b> Reverse Osmosis operation. ....	10
<b>Figure 2.2:</b> Solar Water Disinfection. ....	12
<b>Figure 2.3:</b> Ceramic water filter with receptacle. ....	14
<b>Figure 2.4:</b> Test bar shape used for tensile stress test. ....	20
<b>Figure 2.5:</b> Stress-Strain Diagram for Ceramic Composite Phases. ....	22
<b>Figure 3.1:</b> a) PDMS Silicone Elastomer QSIL 216, b) PDMS Silicone QSIL 216, c) Syringes, Petri dish, spatula, stirring rods, and d) Original Prusa i3 MK3 3D printer. ....	23
<b>Figure 3.2:</b> a) Pounded Birsana bark into smaller crumps, b) Nyennol bark pounded into smaller crumps. ....	25
<b>Figure 3.3:</b> Mould Designs: a) Rectangular mould and b) Cylindrical mould. ....	28
<b>Figure 3.4:</b> a) measuring of the herbs b) soaking of the herbs overnight c) strained solution ready for quenching. ....	30
<b>Figure 3.5:</b> Sample Preparation: (a) Dogbone mould designed on SolidWorks and (b) 3D printed using Prusa i3 Mk3s. ....	31
<b>Figure 3.6:</b> PDMS-Based Membrane Preparation: (a) Grinded salt with PDMS cast on it (b) Sugar cubes with activated carbon and PDMS cast on it (c) Sugar cubes leached in water (d) Foam structure formed after leaching of sugar cubes, and (e) PDMS membranes with activated carbon for the filters. ....	32
<b>Figure 3.7:</b> a) The Solidworks design of the filter container b) the 3D printed filter container with the PDMS membrane in it. ....	33
<b>Figure 3.8:</b> Sample Preparation: (a) Sieved Banana Peels and (b) Sieved Orange Peels. ....	34
<b>Figure 3.9:</b> The activated carbon preparation process: (a) Coconut coir washed with distilled water, (b) Coconut fibre soaked in 10% KOH solution overnight, (c) Dried coconut coir burnt at 300 degrees temperature in a furnace, (d) Carbon obtained after burning, (e) Carbon obtained after burning, and (f) Dried Activated Carbon. ....	35
<b>Figure 3.10:</b> 3D Activated and agriculture waste filters. ....	36
<b>Figure 3.11:</b> The ceramic filter design in Solidworks and it dimensions. ....	36

<b>Figure 3.12:</b> Proposed Final Design of the filtration system: Schematics of the Assembled Filters, (b) Details of the Ceramic Section, and (c) Fabricated System.....	40
<b>Figure 3.13:</b> Three-point bend set-up for flexural modulus test.....	44
<b>Figure 3.14:</b> Flexural Testing: a) Pasco machine with sample, b) sample at the point of fracture, c) three samples showing failure occurring at 45 degrees, and d) rectangular sample for three-point bend test.....	45
<b>Figure 3.15:</b> PDMS Sample under Tensile Test.....	46
<b>Figure 3.16:</b> Determination of Porosity and Density: a) set-up of samples in water, b) saturated samples, and c) saturated samples left on paper towel for droplets of water to dry before measurements.....	47
<b>Figure 4.1:</b> Load analysis simulation on the steel structure. (a) Displacement, (b) Strain, and (c) Stress Analysis.....	49
<b>Figure 4.2:</b> Graph to determine the flow rate of the agricultural waste and activated carbon filter.....	50
<b>Figure 4.3:</b> A graph showing the turbidity, pH and conductivity of the three water samples before and after filtration with granular activated carbon, compared with the WHO standard: (a) River Densu, (b) Nana Mall River, and (c) River Abandza.....	52
<b>Figure 4.4:</b> A graph showing the turbidity, pH and conductivity of Nana Mall Water sample before and after filtration with locally activated carbon, compared with the WHO standard.....	53
<b>Figure 4.5:</b> A plot showing the density and apparent porosity (%) of the different clay-sawdust ratios: (a) Density, (b) Apparent Porosity, and (c) Relationship between Density And Apparent Porosity of the Samples.....	54
<b>Figure 4.6:</b> Nana Mall Water Filtration with Ceramic Filter from the Different Clay-Sawdust Ratios: (a) Conductivities of water filtered, (b), pH of Water Filtered, (c) Turbidity (NTU), and (d) the Turbidity of Water Filtered from the Different Clay-Sawdust Ratios.....	56
<b>Figure 4.7:</b> Stress-strain curve for a 5:1 PDMS sample.....	58
<b>Figure 4.8:</b> (a) leached sugar cubes, (b, c) experimental set up of filtration process (d) foam placed in bottle cover (e) unfiltered and filtered water.....	59
<b>Figure 4.9:</b> (a) Flow rate graph for 0.5cm thickness (b) Flow rate graph for 1 cm thickness.....	60

**Figure 4.10:** Effect of PDMS Membrane Film Thickness on Water Quality: (a) pH of the water  
(b) conductivity (c) Turbidity. .... 61

**Figure 4.11:** Flow Rate and Water Quality Obtain from PDMS Membrane Film: (a) Volume of  
Water Collected versus Time, (b) Data from River Abandza Water, (c) Data from River Densu,  
and (d) Data from Nana Mall River..... 62

**Figure 4.12:** Graph showing turbidity, conductivity, and pH of the filtrate water from the entire  
filtration system. .... 63

## **List of Tables**

<b>Table 2.1:</b> Some Maximum Permissible Composition of Heavy Metals in Drinking Water.....	8
<b>Table 3.1:</b> The estimated weights applied on the steel structure. ....	41
<b>Table 4.1:</b> Data Obtained from Experiment to measure flow rate of Activated carbon filter.....	50
<b>Table 4.2:</b> Water Quality Test for Control Test. ....	52
<b>Table 4.3:</b> Water Quality Analysis Results for Locally Made Activated Carbon.....	53
<b>Table 4.4:</b> Peak Loads and Extension Displaced by PDMS-Matrixes.....	58
<b>Table 4.5:</b> Ultimate Tensile Strength values obtained from Stress-Strain curves. ....	59
<b>Table 4.6:</b> Heavy Metal Concentration in Nana Mall Before and After Filtration.....	64

# CHAPTER ONE

## 1.0 Introduction

### 1.1 Background

Water is an essential requirement for the survival of all life forms, complementing our basic needs such as food production and contributing to socio-economic growth [1]. The importance of water cannot be overemphasized, and hence, safe drinking water is essential. The World Health Organization (WHO) defines safe-drinking water as water that poses no significant risk to health over a lifetime of consumption, taking different sensitivities between life stages [2,3]. Individuals, governments, and organizations are making strides every day to increase access to clean drinking water. Globally, 785 million people lack a primary drinking water service, including 144 million people who depend on surface drinking water [4]. In Ghana, most surface water bodies are polluted, about 66% of the citizens lack access to safe drinking water [5]. Lack or inadequate supply of clean drinking water exposes people to diseases such as diarrhoea, dysentery, typhoid, and cholera [4,6,7]. Children under the age of five are the most vulnerable, with an estimated 800,000 deaths each year [8,9].

Water contaminants can be classified as organic, inorganic, biological, or radioactive. Nature's and humans' activities can both pollute surface water. Natural water pollution sources include rainstorms/wind, floods, soil erosion, bushfires, etc. Farming along with riverbanks causes damming rivers with sand/clay, resulting in high water turbidity and the need for water filtration before human consumption/for domestic use. Water pollution in Ghanaian communities is primarily caused by activities such as poor farming practices and illegal mining ("Galamsey")/small-scale mining practices [6]. The inorganic pollutants include heavy metals which are toxic even at low concentrations, such as Arsenic, Mercury, Copper, Beryllium,

Chromium, and Lead [10]. Some of these heavy metals, such as Mercury, end up in water bodies because of their use in Ghana's illegal mining. Pesticides, residential garbage, and industrial wastes, among other things, are major anthropogenic causes of organic pollution [10]. The presence of live organisms such as algae, bacteria, protozoa, or viruses causes the biological pollution of water [11].

## **1.2 Demand for Quality Water**

In Ghana's Northern Sector (Northern Region, Savannah Region, Upper West Region, Upper East Region, and Northeast Region), approximately 40% of the population gets their drinking water from contaminated sources [5]. This has resulted in water-borne diseases in the region, the most prevalent of which is Guinea Worm [12]. Sub-Saharan Africa's population growth, urbanisation, and economic growth have increased demands and stresses on water systems. The population is expected to quadruple, from 1.34 billion in 2020 to 2.5 billion by 2050 [13]. Furthermore, only about 56% of city dwellers had access to piped water in 2018 [13].

## **1.3 Problem Statement**

According to the WHO/UNICEF Joint Monitoring Programme, improved water sources are free from external contamination, particularly faecal matter, by way of their construction [7]. Examples include standpipes, boreholes, protected dug wells, springs, and rainwater collection [6]. Globally, 1.8 million people die each year due to water-related diseases. In 2000, Ghana recorded about 10,000 - 20,000 deaths due to a lack of clean water [14]. Activities of farmers and illegal mining significantly affect water quality; the chemicals used in fertilizers and weedicides contaminate water. In small-scale or illegal mining, heavy metals such as mercury, lead, copper,

and arsenic are essential but toxic to humans [15]. As of 2018, access to improved water sources in Ghana was estimated at 89%, with 93% urban coverage, and 84% rural coverage [7]. Population growth and increased economic activities continue to stress the existing water resources, and continuous effort in terms of funding and maintenance is needed to maintain good water quality to ensure a continuous supply. It is incumbent to see the need to devise a sustainable, easily maintained solution to provide safe drinking water for all using available raw materials. Hence, the inhabitants of rural communities in Ghana mainly need an effective way of treating water for drinking by increasing efficiency in particulate removal, odour, heavy metals, and bacteria from polluted water.

#### **1.4 Motivation**

The motivation for this work stemmed from the need to optimize water filtration processes using available materials. The motivation for creating an optimized ceramic filter stems from the traditional pottery making process in Ghana. Women in the northern sector of the country are well-known for making pots of various sizes that are strong enough to hold water and cook for an extended period while maintaining structural integrity. They do not allow the pots to cool naturally after baking but rather quench them in a herb-infused chemical solution. However, the plants' content, concentration, and composition are unknown. The goal is to characterize the herbs and replicate the formula in the laboratory by creating a quenching medium for quenching ceramic filters for effective water filtration.

Furthermore, agricultural waste, such as orange peels and banana peels, is a nuisance to our environment, but it has the potential to be used to remove heavy metals. It is estimated that in Ghana, the total area of oil palm trees is about 330,000 hectares [16], and more than about 3,600



hectares are coconut trees [17]. By-products such as coconut and palm kernel shells are good resources to produce activated carbon for effective particulate and odour removal. Two Ashesi University alumni (Kofi Addae-Boahene and Lartey Lesley) have already laid the groundwork for the design of water filtration systems; however, some water quality test results did not meet WHO guidelines. As a result, the goal of this project is to improve on what has already been done.

### **1.5 Goals and Specific Objectives**

The overall goal of this project is to design and optimise a water filtration system for effective particulate and heavy metal removal. The specific objectives for achieving these goals are as follows:

- To conduct field research and collect water samples on current water bodies around the Eastern Region (available to the indigenous people for drinking and domestic use). For example, rivers, streams, boreholes, etc.
- To identify traditional herbs used for quenching clay pots and study their chemical composition.
- To determine the optimum composition of herbal extracts that give optimum structural integrity to the ceramic filter.
- To test the mechanical properties of the ceramic filter and iterate the clay composite until optimum properties are achieved.
- To mould ceramic filter through an optimized process such as shape, porosity, and tapering angle.
- To perform polymerization and biofilter fabrication at different thicknesses with incorporated adsorbates.

- To mechanically characterize the biofilters.
- To perform porosity characterization of the polymer membranes.
- To study the effect of orange and banana peels on heavy metal/particulate adsorption and activated carbon in particulate removal.
- To perform turbidity, pH, adsorptivity, flow rate, and conductivity tests on the filtration system.
- To perform water quality analysis tests before and after filtration. Compare performance with the Environmental Protection Agency (EPA) and WHO limits for drinking water.

## CHAPTER TWO

### 2.0 Literature Review

#### 2.1 Water Contamination

Contamination of water is a problem that affects people all around the world. This can be either geological or anthropogenic (created by humans). Acute health impacts from higher pollutants in drinking water are not rare. Of course, individual susceptibility and form of contact with the body have a role [11] as the geological materials through which groundwater flows. Groundwater moving through sedimentary rocks and soils can pick up a wide range of compounds, including Magnesium, Calcium, Chloride, Arsenate, Fluoride, Nitrate, and Iron. The impact of these natural contaminations is dependent on their types and concentrations. Water can also be contaminated by naturally occurring elements present in unacceptable amounts. Contaminated water has the presence of heavy metals that are harmful to human health. These metals are Arsenic, Chromium, Mercury, Antimony, Lead, and Cyanide [11]. Different research papers categorized pollutants in water differently; however, dominant categorization centered on pollutants caused by natural contaminants, artificial by-products, and human activities. These pollutants can be characterized into inorganic, organic, biological, and radiological categories.

##### 2.1.1 Inorganic Contaminants

There are several inorganic substances found in water. Their chemical parameters can measure the presence of these contaminants. Inorganic contamination of the aquatic environment is generated by naturally occurring compounds (Fluoride, Arsenic, and Boron), industrial waste (heavy metals such as Mercury, Cadmium, Chromium, and Cyanide), and drinking water distribution systems (Aluminium, Copper, Iron, Lead and Zinc) (*Table 2.1*). Natural inorganic

minerals primarily pollute groundwater. Industrial and agricultural waste primarily pollutes surface water, such as rivers, lakes, and ponds. Distribution system pipes pollute tap water [18]. These inorganic pollutants are heavy metals, radioactive materials, and inorganic anions [18].

### **2.1.2 Heavy Metals and Effects on Human Health**

Heavy metals generally enter the aquatic environment through atmospheric deposition, erosion of geological matrix, or anthropogenic activities caused by industrial effluents, domestic sewage, and mining wastes [19]. Iron, Zinc, Fluoride, Copper, Chromium, Iodine, Cobalt, Molybdenum, and Selenium are trace elements recognized by the WHO as essential for human health, but only in small amounts. They can be detrimental when consumed in large quantities. Silicon, Manganese, Nickel, and Boron are examples of metals harmful to human health [20]. There are numerous harmful metals exposed to the environment in Ghana, both in urban and rural communities. When released into the environment, these toxic metals may end up in surface water bodies or percolate into the soil, polluting underground water [21].

Some of the effects of heavy metals in drinking water are problems with blood composition, which affect the kidneys and liver, causes regular fatigue and damage to mental functions [22]. More fatal effects of long-term exposure to heavy metals in drinking are diseases such as Alzheimer's disease, Parkinson's disease, and Sclerosis [23]. Fluoride enters the brain, allowing aluminium to pass through the blood-brain barrier, raising the risk of many disorders. Excessive fluoride amounts (Environmental Protection Agency, EPA 4.0 mg/L) have been found in groundwater in over 20 developed and developing countries, including India, where 19 states were experiencing acute Fluorosis [11]. **Table 2.1** illustrates some heavy metals and their EPA limits.

**Table 2.1:** Some Maximum Permissible Composition of Heavy Metals in Drinking Water.

<b>Heavy metals</b>	<b>EPA limits for drinking water (ppm)</b>
Arsenic	0.01
Barium	2
Cadmium	0.005
Chromium	0.1
Lead	0.015
Mercury	0.002
Silver	0.0001

### **2.1.3 Organic Contaminants**

Pesticides, residential garbage, industrial waste, and other anthropogenic sources of organic contamination are the most common. Organic material contamination can lead to significant health issues like cancer, hormone disturbances, and nervous system diseases [24]. Pesticides are made to interact with the pest's living body chemistry through various chemical mechanisms. Unfortunately, all pesticides may interfere with the metabolism of non-targeted living organisms because of this. Pesticides mainly harm the liver and neurological system. The development of a tumour in the liver has also been reported [11].

### **2.1.4 Biological Contaminants**

Living organisms such as algae, bacteria, protozoans, and viruses create biological water pollution. Each of them can release specific toxins into the water. Some protozoans are commonly found in lakes, rivers, and streams contaminated with animal faeces or wastewater from sewage treatment plants. diarrhoea, stomach cramps, nausea, exhaustion, dehydration, and headaches are

possible side effects. Viruses are the tiniest living entities capable of infecting others. Hepatitis and polioviruses are commonly reported in contaminated water [11].

### **2.1.5 Radiological Contaminants**

Radioactive sources cause radiological contaminants. Some common natural radioelements are those from the uranium-238 chain, a natural radioactive series of many radionuclides, one descending from the other. All types of radiological contamination increase the risk of cancer [11].

## **2.2 Water Treatment Techniques**

Water filtration is known to have been in existence for about 4000 years now [25]. The main aim was to ensure water was physically clean; however, it was soon realized that this did not mean the water was safe to drink [25]. Over the years, there have been many ways of treating water, such as boiling. However, the invention of microscopes brought the innovation of a multi-stage filter [25]. There are various methods of water filtration. Some of the filtration processes used now are activated carbon, reverse osmosis, and heavy water removal.

Point-of-use (POU) technologies are on-site water treatment and storage facilities that aid in the removal of pathogens from water before consumption [26]. POU water treatment technologies are low-cost, low maintenance, user friendly and grid-independent. Also, they are simple, acceptable, low-cost interventions at the household and community level that can remove microbes from water without a centralized water treatment and distribution system [27,28]. POU water treatment techniques, which improves drinking water quality at the household level, provide a cost-effective and convenient way to obtain safe drinking water, potentially reducing outbreaks of waterborne

diseases [29,30]. The current state of several POU-water purifying approaches was investigated, filter press technologies were reviewed, and specific functional requirements for an appropriate and cost-effective filter press were identified. Cloth filtration, boiling, chlorination, solar disinfection, bio-sand filters, and ceramic water filters were among the POU filtration technologies.

### 2.2.1 Reverse Osmosis

Reverse osmosis refers to a water purification process which uses a semi-permeable membrane to remove ions, molecules, and larger particles from contaminated water (*Fig. 2.1*). This technology has been present for over fifty years and is widely used in industrial operations and is a credible way of treating water [31]. This water filtration method can be used to filter dissolved salts, mostly from seawater and other particles such as debris in the feed water [31].

This is done with an applied pressure to push the feed water through the semi-permeable membrane technology, thus, filtering out the contaminants. Using reverse osmosis, heavy metals such as Zinc, Cadmium, and Copper are usually removed from polluted water.

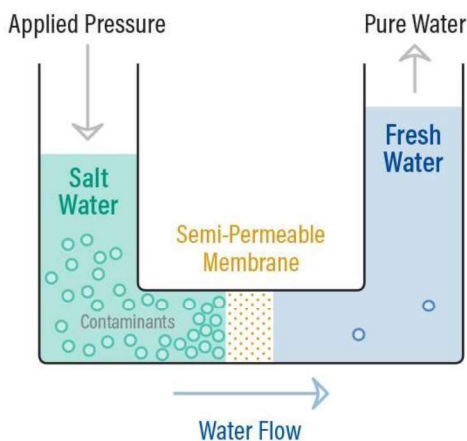


**Figure 2.1:** Reverse Osmosis operation [32].

### **2.2.2 Activated Carbon Adsorption**

Granulated Activated Carbon (GAC) is a frequently used filtration material [33]. It can remove organic and residual disinfectants in water [33]. GAC has numerous benefits when included in the filtration process of water; thus, including it in the main filter is vital. The significant advantage of GAC is its ability to improve the taste and odour of filtered water and reduce the risk of a person getting ill from drinking the water [33]. The activated carbon (AC) removes the contaminants from the water by adsorption. Adsorption occurs when the molecular forces of a solid surface come into contact with a fluid, the solid then attracts the molecules or ions of the fluid to itself [34]. Due to the granular nature of the carbon, it is porous with tiny holes between each particle, making the filter very effective. The AC then adsorbs these contaminants in the water, thus, giving the filtered water low turbidity, good taste, and no odour. AC protects the other components used in the filtration process from possible damage by oxidation [33]. Continuous exposure of the contaminants to the filter units, such as the reverse osmosis membranes, can damage these units. AC is made from common raw materials found in any Ghanaian community. Some raw materials used are wood, coconut shells, palm kernel shells, rice husk, sawdust, etc [34]. The surface area for activated carbon depends typically on the raw materials used. However, the average surface area for activated carbon is 1000 square meters per gram [33].

### **2.2.3 Solar Water Disinfection**

This is also known as solar disinfection (SODIS), a technique developed in the early 1980s. Contaminated water is placed in transparent bottles. Bottles are filled, agitated to oxygenate them, and then placed on a roof for six hours to expose them to the Sun. The relatively widespread usage



of old bottles is a disadvantage of SODIS. Light transfer and overall SODIS effectiveness are reduced when used bottles have scratches. Furthermore, the clarity of the plastic is affected by bottle labels or their residue, and SODIS' disinfection efficacy is diminished. The leaching of plastic bottle material into the water and the regeneration of bacteria previously grown in the water bottle are both critical problems with this procedure [30].

For UV disinfection, SODIS (**Fig. 2.2**), and chlorine disinfection to work, the feed water must have low turbidity. However, the turbidity of the water in many of Ghana's dugouts is exceptionally high [35]. Coagulants considerably reduce turbidity and microorganisms in water, but they do not sterilize pathogens. Thus, they must be used with other methods. Cloth filtration can remove the guinea worm-causing bacteria, large particles, and debris, but not turbidity or tiny microbes [35].

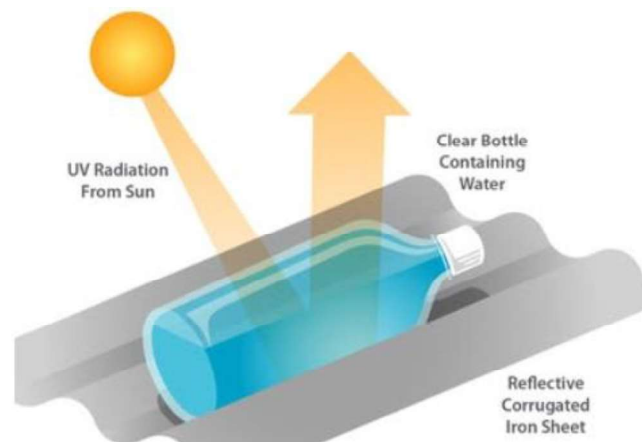


**Figure 2.2:** Solar Water Disinfection [35].

#### 2.2.4 Ceramic Filter Technique

According to [36], ceramic filters can be classified according to their physiological properties. These are shaped (disk, candle element, pot, etc), type of clay (red clay, white clay, etc), combustible material (sawdust, rice husk, flour, etc). Ceramic filters could also be classified by microbial removal, chemical contaminant/heavy metal removal such as arsenic, iron, etc., and

secondary contaminant removals such as taste and odour. Ceramic water filters are point-of-use (POU) water treatment technologies made from locally available raw materials such as clay and sawdust. They can be used to treat water before consumption.

According to [37,38], the microbes responsible for dysentery in developing countries are *Escherichia coli*, *Enterococcus*, *Cryptosporidium*, and rotavirus. The drinking water guidelines by the World Health Organisation (WHO) state the undesirability of any form of faecal coliform in drinking water and connected distribution systems [38]. Ceramic materials have high hardness and strength, are durable, have high melting points and are good insulators. Clay as a ceramic material has been identified for use in ceramic water filters because of its high plasticity and heat resistant properties. Upon controlled heating and cooling, it can develop the needed porosity to be used as a water filter. Ceramic water filters allow water to pass through their porous base while disallowing the passage of potentially harmful microbes [39]. Also, when the treated water is susceptible to recontamination, it is advisable to use a point-of-use. According to [41], clay and sawdust are the commonly used materials for ceramic water filter preparation. Also, the filter's pore size and surface charge determine its ability to remove pathogens and particles from contaminated water [40].

Ceramic water filters are made by mixing clay and sawdust, rice husk or any combustible biomass proportionally into a paste. The paste is shaped into a filter using a press. The filter is then baked in a kiln at a high temperature, during which the biomass burns off, leaving pores in their original places. These pores are big enough to allow water to pass through but small enough to prevent microbial penetration. Ceramic filters can remove between 97.86% and 99.97% *E. coli* [39]. Also, the filter can remove particulates and protozoa, and coating the filter with colloidal silver can increase *E. coli* removal efficiency to up to 100% [39].

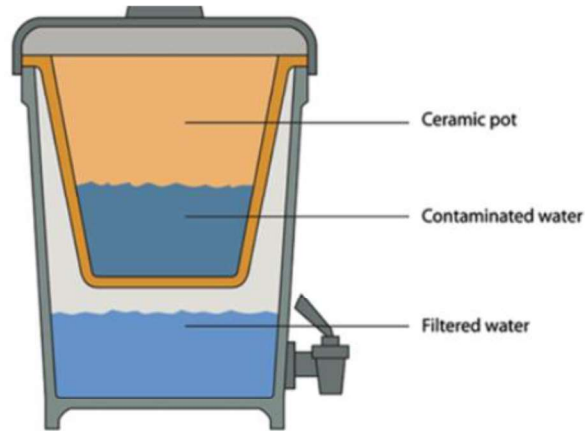


**Figure 2.3:** ceramic water filter with receptacle [41].

### 2.3 Description of the Poly-dimethyl-siloxane

Polydimethylsiloxane (PDMS) is a polymer that belongs to the group of silicone elastomers [42]. It is widely used in mechanical and electronic components due to properties such as resistance to corrosion, flexibility, chemical stability, biocompatibility, and low cost [42]. This elastomer is easy to manufacture and is transparent, hence, its wide use in industries [42]. In microfluidics, PDMS has been seen to be very effective compared to the old techniques that involved the use of glass and silicon, and it has relatively higher properties such as its resistance to corrosion and biocompatibility [43,44]. Other properties which make PDMS a good resort for filtration are its permeability and elasticity [45]. The biocompatibility property of PDMS makes it a good resort for filter membranes. This biocompatibility feature means that PDMS will be compatible with biological tissue [42]. Some of these biological tissues may be found in the ground, such as *parenchyma* and *collenchyma*. Thus, when used as a filter, it will not react negatively with the bacteria in the water to become toxic, thus polluting the filtered water. Another essential feature of PDMS is its optically transparent feature, making it easy to track contaminants [46].

## 2.4 Flow Properties

### 2.4.1 Porosity

The volume of voids in a solid is divided by the total volume of the solid to determine its total porosity. Since porosity measures, the volume of space in a solid, filters showing a greater porosity will allow more water to pass through them. However, increasing the pore size during filtering may compromise the mechanical screening phenomenon [47]. For a ceramic filter, it is critical to keep sawdust particle sizes under 1 mm. According to the literature, the pore diameter of most ceramic water filters is between 0.2 and 2.5 microns [47]. In certain production areas, filter mix ratios are adjusted to achieve acceptable flow rates ranging according to the particle size of rice husks or sawdust.

The pore size distribution of a ceramic filter sample can be calculated using Image J software on the High-resolution scanning electron microscope (HRSEM) image. The HRSEM is a cutting-edge imaging system for studying the morphology of surfaces down to the nanoscale [48]. The average pore size ( $d$ ) can be evaluated using the following formula:

$$d = \sqrt{\frac{\sum_{i=1}^n n_i d_i^2}{\sum_{i=1}^n n_i}} \quad (2.1)$$

where  $n_i$  and  $d_i$  are the pore diameter and number of pores respectively [49].

The porosity of the ceramic filter could also be determined using the water absorption test (direct) method. The apparent porosity can be calculated using the expression:

$$p = 100 \left[ \frac{W_{saturated} - W_{dry}}{W_{saturated} - W_{underwater}} \right] \quad (2.2)$$

where  $W_{\text{saturated}}$  is the weight of the specimen when saturated in water,  $W_{\text{dry}}$  is the weight of the dry specimen and  $W_{\text{under water}}$  is the weight of the sample underwater [50].

#### **2.4.2 Flow rate and Turbidity**

The turbidity of water refers to the level of suspended particles in it. The flow rate of the water and its turbidity are indirectly proportional. The higher the level of suspended particles in a water, the lower the flow rate. This is caused by the clogging of the pores of the filter's membrane during filtration [51]. The turbidity of water is measured using a turbidity sensor (nephelometer), and the unit is Nephelometric Turbidity Units (NTU). According to the WHO, the required turbidity of drinking water is ideally below 1 NTU and should not exceed 5 NTU [45]. The formula gives the flow rate of the filtration:

$$Q = \frac{V}{t} \tag{2.3}$$

where  $V$  is the volume of the water that is filtered,  $t$  is the time it takes for the water to be filtered.

#### **2.4.3 Permeability and Tortuosity**

Permeability measures the relative ease with which water molecules can pass through porous ceramics. On the other hand, tortuosity reflects the likelihood of pollutants being captured. The permeability correlates with the total porosity, whether the pores are closed, isolated, or interconnected. The permeability of a porous material is usually expressed using the interconnected pore sizes and physical properties of that material, which are the tortuosity and porosity [53].

On the other hand, tortuosity is due to the path taken by the water molecules. Tortuosity of the material ranges from 10 to 60. A tortuosity rating of 10, for example, means that a particle travelling through water molecules must travel through an effective length ten times the actual length (or thickness) of the ceramic water filter to pass through. The fitting of flow rate data can determine the permeability value to the Darcy equation at a high R-square value [47]. Darcy's equation is of the form [47].

$$Q = \frac{KA \Delta P}{\mu L} \quad (2.4)$$

where Q is the water discharge from the porous media, A is the surface area that contains the water,  $\Delta P$  is the change in water head due to gravity flow, K is the porous structure's hydraulic conductivity, and L is the thickness of the porous media that the water must percolate through [51].

The hydraulic conductivity, K, has the formula:

$$K = \frac{\gamma k}{\mu} \quad (2.5)$$

where  $\mu$  is the viscosity of water at a given temperature,  $\gamma$  is the specific gravity of water at that temperature and k is the intrinsic permeability of the porous media, which defines its porosity and interconnectivity [51].

## 2.5 Microbial and Virus Removal

### 2.5.1 Microbial Removal

Aside from chemical contaminants, pathogens such as bacteria (for example, *E. Coli*, *vibrio cholerae*, *C. Coli*, etc.), viruses (examples Adenovirus, Norwalk, Rotavirus etc),

protozoa (E.g *Entamoeba histolica*) are significant causes of the spread of diseases. The effectiveness of the ceramic water filter in microbe removal is mainly due to two mechanisms: mechanical screening and colloidal silver impregnation [47]. Indicator organisms are used to determine removal efficiency. Colloidal silver is a solution composed of colloidal macromolecules and a thermodynamically stable solvent that is simple to reassemble after the macromolecules are separated from the solvent. Using colloidal silver as a disinfectant in ceramic filtration stops bacteria from growing in the filter and improves bacteria inactivation [54]. In India, ceramic candle filters were soaked in silver salts with a pore size of 6-31 microns and a filtration rate of 3-4 litres per hour. This method produced bacteria-free filtered water [55].

### **2.5.2 Virus Removal**

Due to the small size of viruses, virus removal with ceramic water filters remains a challenge. Virus deactivation has not been successful with silver, used to treat germs. It has also been discovered that the log removal value (LRV) of male-specific (MS2) bacteriophages is modestly reduced in filters treated with colloidal silver, implying that colloidal silver does not have a good effect on virus eradication [47]. However, ceramic water filters do not effectively remove MS2 bacteriophages in filters with or without colloidal silver [56]. Resource development international (RDI) adds laterite, an iron-oxide rich compound, to their filter mix as it is thought to provide additional viral binding sites. However, although 1-2 logarithm ten reductions (90-99%) in MS2 was documented, no significant difference was found between filters with or without laterite [57].

Ceramic pot filters would need to achieve at least 3 LRV for viruses, as demonstrated by MS2 and phiX174 [58], to qualify as protective in WHO's verification scheme for household water

treatment systems. Reported MS2 reductions reached almost 3 LRV after 13 weeks of continuously filtering canal water through ceramic pot filters [59], which was hypothesized to be due to the growth of biofilms on the filter during operation.

## **2.6 Mechanical Properties**

### **2.6.1 Elasticity**

Elasticity refers to a material's ability to return to its original shape after removing a load. Due to the Si-O structure of silicones, they have good elastic capacity and are more flexible than other conventional polymers with C-C carbon structures [45]. The ability of adjacent polymer areas to glide on each other determines the polymer's elasticity. The number of existing cross-links influences this feature; the more cross-linked the PDMS is, the less elastic it will be [45]. PDMS is prepared by mixing a prepolymer with a cross-linker at a weighted ratio, normally 10:1 [60].

### **2.6.2 Stress and Strain**

Stress refers to the force acting on material over its surface area.

$$\text{Stress, } \sigma \text{ (MPa)} = \frac{F}{A} \quad (2.6)$$

where F is the force used to stretch the material, and A is the test section surface area of the specimen. The test bar that is to be used for the tensile stress test has the shape of a dogbone, with the broader end sections attached to the test apparatus and the thinner shaft forming the actual test section [60].



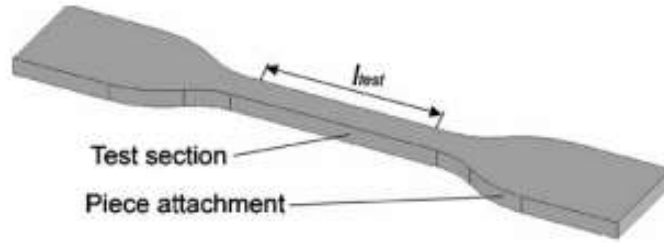


**Figure 2.4:** Test bar shape used for tensile stress test [60].

Strain refers to the change in the length of material over the original length of the material.

$$\text{Strain, } \varepsilon = \frac{\Delta L}{L_0} \quad (2.7)$$

where  $\Delta L$  is the change in length of the PDMS specimen,  $L_0$  and is the original length of the PDMS specimen.

### 2.6.3 Composite Design

The rule of the mixture was employed in the design of ceramic composite materials. The method is used to approximate the estimation of composite material properties. It is used to predict the stiffness of a composite based on the volume fractions of the constituents (i.e., fibre and matrix) and their corresponding stiffness [61]. The rule of mixtures equations predict that the elastic modulus should fall between an upper bound represented in equation 2.3.

Assuming that all the fibres are aligned in one direction, the stiffness of the composites can be calculated as follows [61]:

$$E_c(u) = (E_f \times V_f) + (E_m \times V_m) \quad (2.8)$$

and a lower bound, or limit

$$E_c(l) = \frac{E_m E_p}{V_m E_p + V_p E_m} \quad (2.9)$$

where  $E_f$  is the stiffness of the fibers,  $V_f$  is the volume fraction of the fibres,  $E_m$  is the stiffness of the matrix and  $V_m$  is the volume fraction of the matrix.

The Flexural Strength is given by [49]:

$$F_s \text{ (MPa)} = \frac{3Fd}{2el^2} \quad (2.10)$$

where  $F$  is the force (N),  $d$  is the distance between the supports,  $e$  and  $l$  are the thickness and width of a rectangular specimen (mm), respectively. The tensile strength is characterized by [49]:

$$T_s = \frac{2F_T}{\pi Dh} \quad (2.11)$$

where  $F_T$  is the force,  $D$  and  $h$  are the diameter and height of the specimen (mm), respectively [49].

From a compressive test, the stress-strain curve reveals the structural properties of a composite material under compression. A typical stress-strain curve a ceramic composite under test is shown **(Fig. 2.5)**.

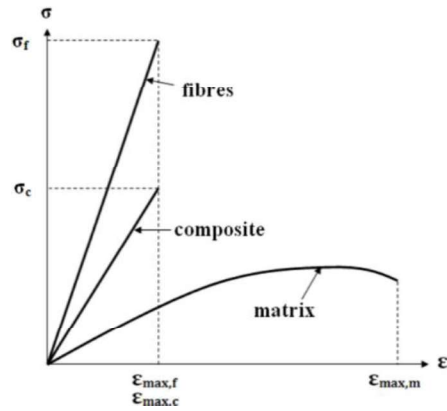


**Figure 2.5:** Stress-Strain Diagram for Ceramic Composite Phases [62].

## 2.7 Scope of Work

The first chapter of this project presents background studies on water pollution and its consequences, problem statement, motivation, and project goals. A review of the literature on related works is presented in the second chapter. Unresolved issues were identified for improvement. The third chapter presents the design requirements, materials selections, and methodologies. This chapter clearly presents 3D models of the filtration system, materials testing, and prototypes for evaluation. The fourth chapter of the report presents the results and discussion section. The implications of the study were aligned with the outcomes of the studies. The final chapter summarises major findings and recommendations for future works.

## CHAPTER THREE

### 3.0 Materials and Methods

#### 3.1 List of Materials

PDMS Silicone Elastomer QSIL 216 (**Fig 3.1a**) and PDMS Silicone QSIL 216 (**Fig 3.1b**) curing agent (cross-linker), the activated carbon, and Kinetic Degradation Fluxion (KDF) filter were purchased from amazon.com. Syringes, Petri dish, spatula, stirring rods, etc. were purchased from FINAP, a chemical Lab around Circle, Accra). Polyvinyl chloride (PVC) pipes, plastic taps, veronica buckets, and other plumbing equipment were procured from Accra shops. Sensors such as the pH sensor, turbidity sensor, water level sensor, license SolidWorks (2018), and the Original Prusa i3 MK3 3D printer (**Fig. 3.1c**) were provided by the Ashesi Engineering Department.

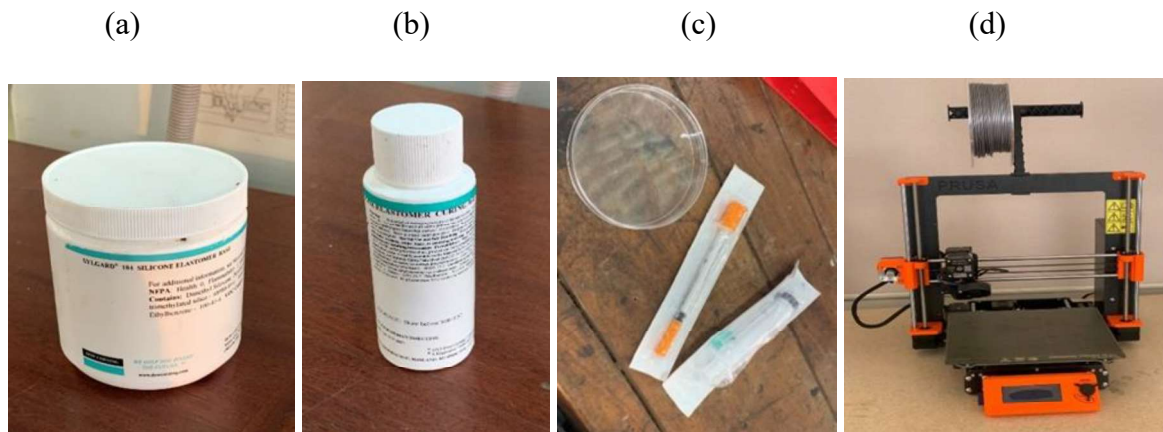


**Figure 3.1:** a) PDMS Silicone Elastomer QSIL 216, b) PDMS Silicone QSIL 216, c) Syringes, Petri dish, spatula, stirring rods, and d) Original Prusa i3 MK3 3D printer.

## **3.2 Ceramic Filter Materials**

### **3.2.1 Clay**

Clay forms the base material of the ceramic filter element. Clay can be readily accessed in most locations Worldwide. It can be molded easily with the right approach. When fired in a kiln, it changes chemically to become a strong, slightly porous container that does not deteriorate in water [47]. A conventional clay pot substantially facilitates the slow passage of water via naturally occurring holes between the platelets of fired clay. The ceramic pot can strain most bacteria, protozoa, helminths, soil, sediment, and organic waste, depending on the size of the pores [47]. In this project, sawdust was used as the combustible material in the clay pot to create pores of similar sizes for testing. Clay acts as the matrix for the ceramic composite. White clay was obtained from the Savannah Region Ghana (in a village called Konkoripe under the Sawla-Tuna-Kalba District). The addition of water and kneading converts the clay into a paste capable of being moulded into the needed shape. Pre-processing of clay includes pounding into powder form and sieving to remove impurities such as debris, small rocks, lumps etc. After this, the clay is ready to be mixed with the burnout material and further processed.

### **3.2.2 Burnout Material**

The burnout material is an organic residue that is combusted during the firing of the ceramic filter to produce pores. Materials such as sawdust, rice rusk and peanut shells can be used. In this project, the burnout material used was sawdust. The sawdust was obtained from a mill in Pokuase, Ghana. The sawdust was checked for quality, and extra materials such as stones and dirt are picked out. It is sieved to obtain uniform texture and ensure that similar pore sizes are created in the ceramic filters when burned out.

### 3.2.3 Traditional Herbs

Additional materials needed are the herbs used to prepare a quenchant. These include two herbs, Biršana and Nyen-nyol (names presented in Birifor language), obtained from the Savannah Region of Ghana (in a village called Konkoriye under the Sawla-Tuna-Kalba District). The barks of both herbs were obtained, pounded and dried for storage. Measured proportions of both herbs were soaked overnight and used to quench the ceramic filter. The solution can also be boiled to speed up the process.



**Figure 3.2:** a) Pounded Biršana bark into smaller crumps, b) Nyen-nyol bark pounded into smaller crumps.

## 3.3 Requirements of the Filtration system

### 3.3.1 Design Requirements

1. The system should be able to produce zero coliform forming units(cfu) per 100 millilitres of water.
2. Turbidity levels should reduce to a maximum of 5 NTU.

3. Microbial removal rates should range from 95% - 99.99%.
4. The system should be able to produce clean drinking water within a reasonable contact time of 0-4 hours.
5. The stand support for the filtration system should be able to support a mechanical load of about 1kN.
6. The filtration system must filter about 6-7 litres of water in a 4 hours of water every 24 hours with an average industrial flow rate of 1.448 litres per hour.
7. The optimized ceramic filter should be able to perform about 80% heavy metals absorption, particulates and bacterial removal and deactivation.

### **3.3.2 Functional Requirements**

1. The system should be able to produce clear, odourless and tasteless water suitable for drinking.
2. The system should be able to filter enough water for a family of four.
3. There should be no traces of clay or biomass in the filtered water.
4. The filtrate storage basin must be able to store the filtered water without any contamination.
5. After absorptivity test, the number of heavy metals present in the filtered water should be the same or below the Environmental Protection Agency limit for drinking water.
6. The user's safety must also be ensured anytime he or she uses the filtration system by ensuring that the water quality is maintained with routine testing/checking.
7. The filtrate storage basin must be capable of storing filtered water free of pollution.
8. The PDMS membrane should be able to filter leaked particulates.

9. The final sample of filtered water after testing should be around the Environmental Protection Agency limit for drinking water to ensure the system's functionality.

### **3.4 Preparation of Ceramic Filter**

#### **3.4.1 Ratio and Mixing**

The clay and the sawdust are measured by volume, even though they could be measured by weight. A study on ceramic filters in Nigeria showed that the clay-saw dust ratio of 50-50 produced the best flowrate capabilities [63][64]. However, this configuration was more prone to mechanical failure. Even though the burnout material is sawdust, the study has guided the selection of configurations to be studied. The clay-saw dust (C-S) configurations are 100-0, 60-40, 55-45, 50-50, 45-55. In addition, the mode of cooling is either air cooling or quenching in the herbal solution. In this situation, the air cooling of the fired ceramic acts as the control experiment. The different samples from the two methods were subjected to the same mechanical tests to ascertain if quenching with the herbal solution affects the structural integrity of the ceramic filter.

#### **3.4.2 Soft Working**

The clay mixture was soft worked (cold worked) to generate plasticity before moulding. The mixture can be kneaded, thrust, or wedged [65]. The mixture is pounded and left overnight, and the process is repeated three times before being compacted into the moulds. The cylindrical moulds have a diameter of 3cm and a height of 7cm. The rectangular moulds have a length of 8cm and a thickness of 2.5cm.



### 3.4.3 Compaction

After undergoing the soft working for three consecutive days, the clay-sawdust mixture was pressed into the moulds (**Fig. 3.2**). Square and cylindrical moulds used for preparing samples for mechanical testing. The moulds consist of a square cross-sectional area and a rectangular length. The sample has a length of  $\sim 7$  cm, a width of  $\sim 3$  cm and a thickness of about 2 cm. The cylindrical moulds are made of PVC pipe of inner diameter of  $\sim 3$  cm and a length of about 7 cm. At least five samples were made for each clay-saw dust configuration. There are two sets of samples; some were air-cooled, and the rest quenched with the prepared solutions. The same applies to the cylindrical samples. The clay-sawdust mixture is added to the mould bit by bit for both square and cylindrical moulds by hand. Then, a rolling pin was used to press the mixture in to ensure there were no voids. Flat metal was used to scrape excesses from the surface of each sample to ensure a flat surface. For the cylindrical mould, a rod-like metal was used to push in the material bit by bit to compact it until the mould filled up. The flat metal was then used to scrape off excess materials. It should be noted that compaction is critical to achieving a good packing density and to avoiding/minimize defects in the sample.



**Figure 3.3:** Mould Designs: a) Rectangular mould and b) Cylindrical mould.

#### **3.4.4 Drying and Firing**

After the clay mixture is pressed into the moulds, they are left in the room to dry slowly for three days. After this, they are placed in the Sun to dry. After drying, the shrinkage of the clay makes it easy to remove from the moulds for further studies. The samples first undergo slow evaporative drying before being exposed to the Sun to avoid rapid drying which could cause cracking.

All the samples were fired using an open-fire charcoal stove (in the absence of a kiln). Firing is done with charcoal with a temperature ranging from 544.6°C to 615.3°C. An electric blower was used to blow warm air upward to burn the biomass within the samples. The samples were fired firstly to strengthen the samples. The firing ensures that the organic material (burnout) is burnt off to produce the porous, spongy structure needed for filtration. However, at the same time, we do not want the clay to keep wearing off into the water that would be consumed. So, the firing is done to prevent this from happening.

#### **3.4.5 Traditional Quenchant Preparation**

The quenching solution was prepared by measuring 100 g of each herb, adding to 2000 ml of water, and leaving the mixture overnight. Before quenching the samples, the herbs were strained out, leaving a clear solution. After firing, the samples were immersed in the solution for about three minutes to allow all bubbles to dissipate.

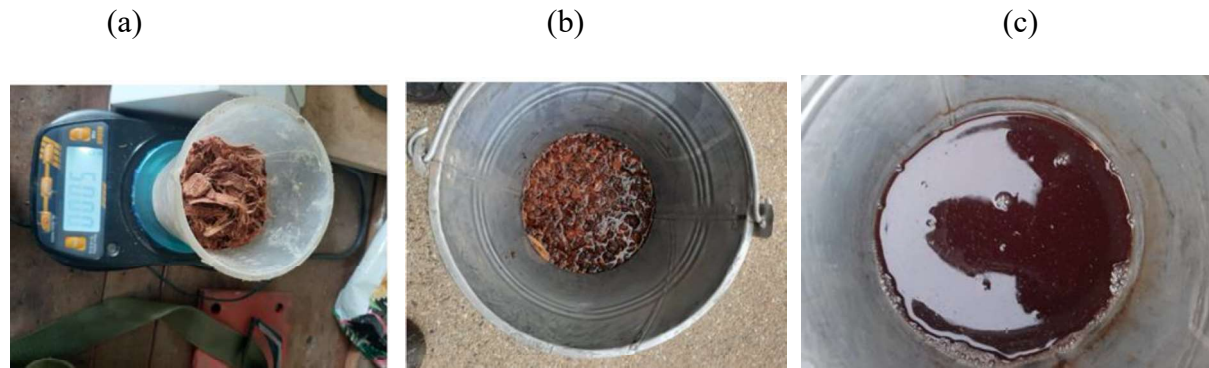


**Figure 3.4:** a) measuring of the herbs b) soaking of the herbs overnight c) strained solution ready for quenching.

### 3.5 Preparation of PDMS Filter Membranes

#### 3.5.1 Curing of PDMS samples

Typically, PDMS is created by combining an elastomer with a curing agent (cross-linker). The mixing weight ratios were 10:1 and 5:1. A 3D model mould was made for a dogbone structure (**Fig. 3.5a**) using Solidworks 2018 version. Slicing software Cura and Prusa i3 3D printer was used to print the mould for the dogbone specimens (**Fig. 3.5b**) at the Ashesi Engineering Department. The PDMS was allowed to dry up in the cast, degassing the bubbles in the PDMS mixture. Due to the unavailability of an oven for this process, a standing fan was used for the degassing. This was left in the workshop for 24 hours, after which the moulds were formed. The moulds (**Appendix F**) formed were then taken out of the dogbone structure for a tensile stress test held in the Ashesi Mechanical Laboratory.

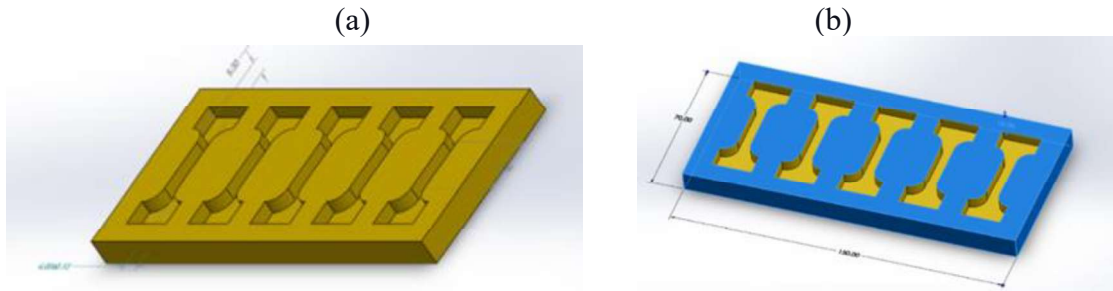


**Figure 3.5:** Sample Preparation: (a) Dogbone mould designed on SolidWorks and (b) 3D printed using Prusa i3 Mk3s.

### 3.5.2 Preparation of PDMS Membrane

Salt was grounded into small particles to create a porous membrane for the filter. The grounded salt was then placed in pipes, and PDMS mixture was then cast onto of the salt or sugar particles to create porous membrane (**Fig. 3.6a**). Also, ground activated carbon was later added to the PDMS mixture before casting to create a PDMS-activated carbon filter membrane to maximize particulate adsorption from the polluted water. The samples were gently removed after 24 hours of curing and leached with distilled water at room temperature.

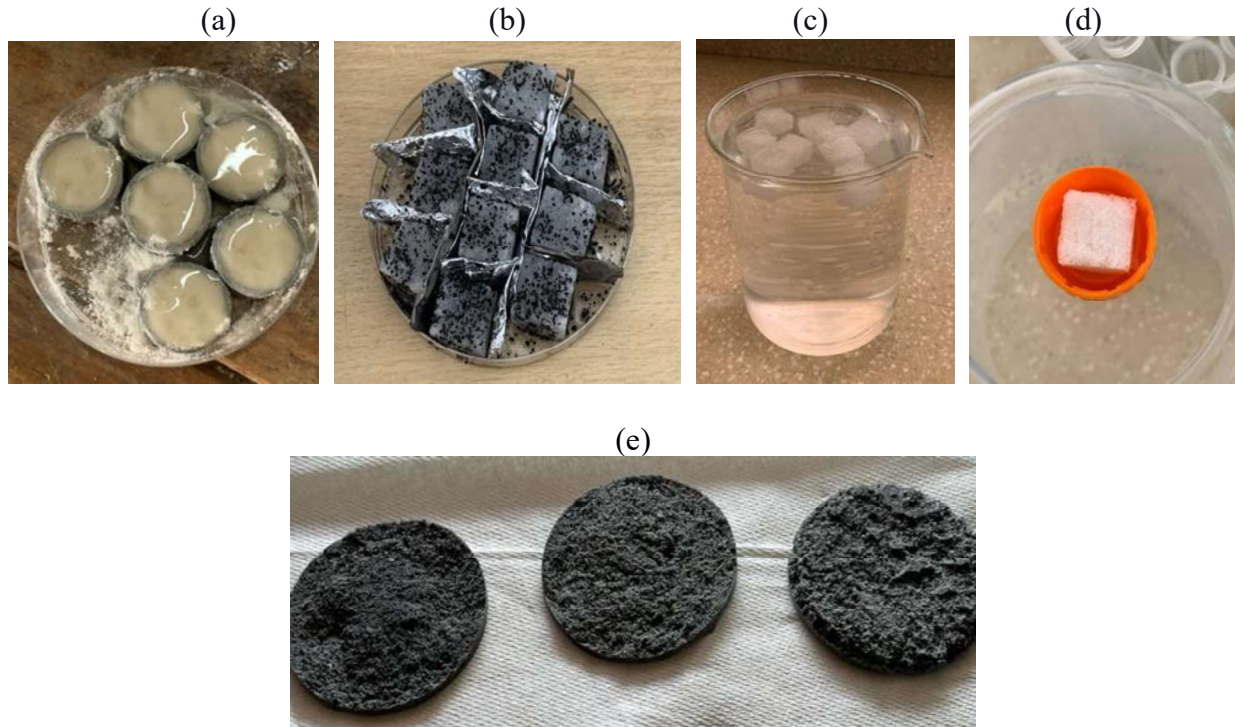


**Figure 3.6:** PDMS-Based Membrane Preparation: (a) Grinded salt with PDMS cast on it (b) Sugar cubes with activated carbon and PDMS cast on it (c) Sugar cubes leached in water (d) Foam structure formed after leaching of sugar cubes, and (e) PDMS membranes with activated carbon for the filters.

### 3.5.3 Fabrication of Filter Container

The filter container was modelled using the SolidWorks 2018 version (**Fig. 3.7a**). The taper angle used for the container is 75 degrees. The filter container was then built using the PLA filament using the Prusa i3 Mk3s 3D printer. The filter body has a height of 9.5cm with an outer diameter of 9.5 cm, and the filter container has a diameter of 10cm. Both the body and container have holes at their centre which have a diameter of 1.45 cm. The print time for this part was just over 22 hours (**Fig. 3.7b**).

Flow rate experiment was set up with the filter container placed on a calibrated beaker to collect filtrated water. A stopwatch was set for every 120 seconds to record the volume of water filtered. The filter is placed under a running tap that is kept at a constant flow rate.



**Figure 3.7:** a) The Solidworks design of the filter container b) the 3D printed filter container with the PDMS membrane in it.

### 3.6 Agricultural waste and activated carbon filter

#### 3.6.1 Preparation of Orange and Banana Peels for Heavy Metal Removal

The preparation of agricultural waste filters begins with acquiring orange and banana peels. These peels were washed with distilled water to remove any lingering dirt that may interfere with filtration. The washed peels were then dried under the Sun for 48 hours. Once this was done, it was finally crushed and sieved at the workshop into final powder orange and banana peels, as indicated in **Figure 3.8**, respectively.



**Figure 3.8:** Sample Preparation: (a) Sieved Banana Peels and (b) Sieved Orange Peels.

### 3.6.2 Preparation of Activated Carbon

Adsorption on activated carbon is superior to other chemical and physical methods for water treatment in efficiently adsorbing a broad range of pollutants [66]. The preparation of the activated carbon begins by soaking washing dried coconut coir overnight in 10% potassium hydroxide solution (**Fig. 3.9a**), followed by washing with distilled water to remove potassium hydroxide and then dried [67]. It is then subjected to activation at 300°C for 30 min in an atmosphere of nitrogen (**Fig. 3.9c**). The carbon obtained is washed with distilled water and 10% hydrochloric acid (**Fig. 3.9c**). The carbon is washed with distilled water to remove the free acid and dried at 105±5°C for 24 h. The carbon was ground to a finer size of 212-500 µm and used in an adsorption test [67].

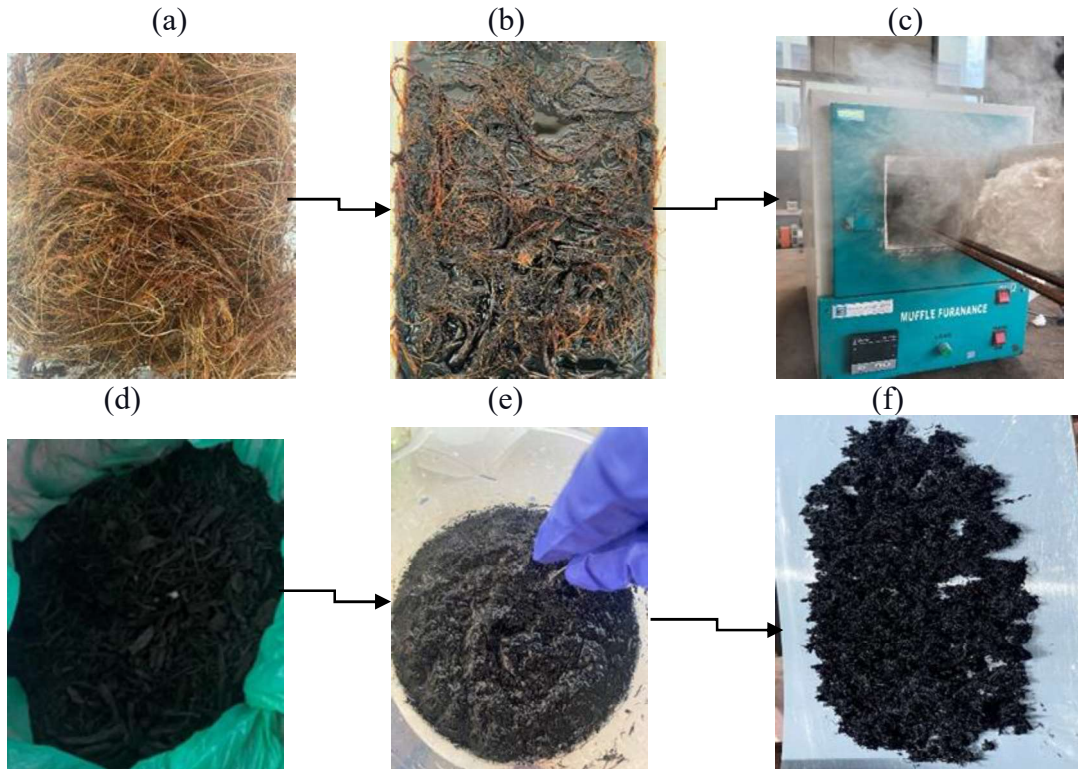


**Figure 3.9:** The activated carbon preparation process: (a) Coconut coir washed with distilled water, (b) Coconut fibre soaked in 10% KOH solution overnight, (c) Dried coconut coir burnt at 300 degrees temperature in a furnace, (d) Carbon obtained after burning, (e) Carbon obtained after burning, and (f) Dried Activated Carbon.

### 3.6.3 Activated Carbon and Agricultural Waste Filter Fabrication

A 3D printed filter was obtained at 35° to enhance flowrate (**Fig. 3.10**). The fabricated filters were loaded with AC and banana and or orange peel, while the bottom section was supported with the PDMS-based membrane. Volumes of water was filtered at regular time interval, while maintaining the level of water in the filter.



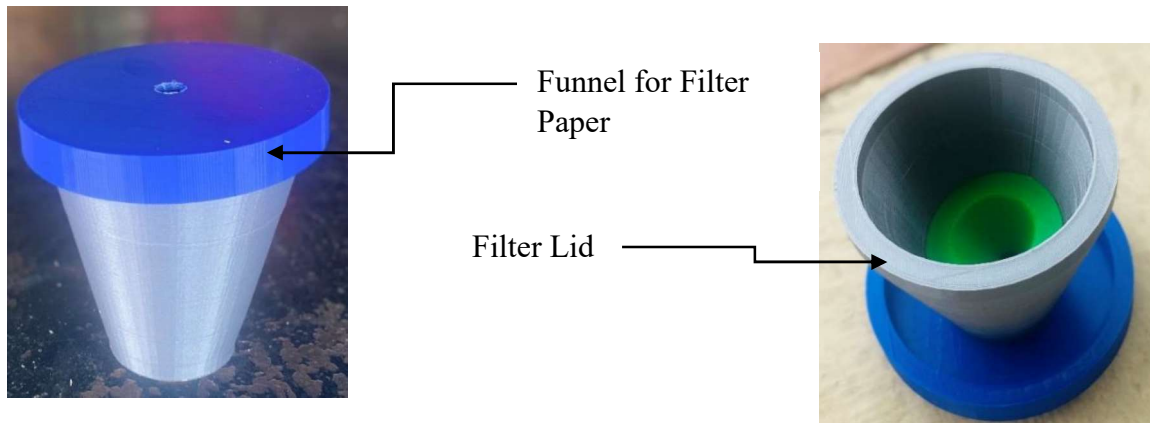


**Figure 3.10:** 3D Activated and agriculture waste filters.

### 3.7 Selection, Sizing and Justification of Subcomponents

#### 3.7.1 Ceramic Water Filter

In a simulation study by Augustus Poku Sarkodie (2021), filters with a height of 20-30 cm with a corresponding taper angle between 10 – 20 degrees proved to be more effective than other combinations; hence the dimensions of the ceramic filter were based on this study. The thickness ranges from 1.5-3 cm (Fig. 3.11) and should be constant throughout the cross-section of the filter. For prototyping and texting, a smaller model was made, which had a height of 14 cm, an open-ended diameter of 10 cm and a closed-ended diameter of 6.5 cm.

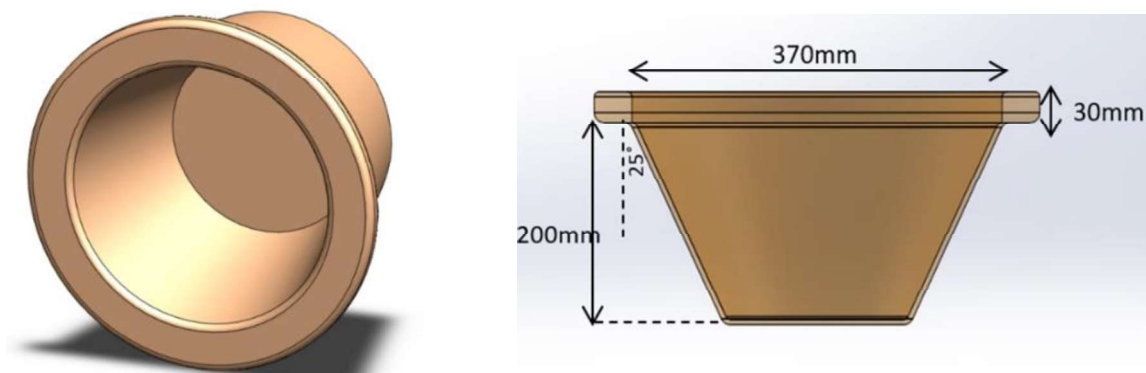


**Figure 3.11:** The ceramic filter design in Solidworks and its dimensions.

### **3.7.2 Submersible Pump and Sizing**

A DC40-1250, Mini submersible centrifugal water pump, DC 12V Brushless Magnetic Drive was used. Submersible pumps are generally efficient because they do not use as much energy moving water into the pump as other pumps do. Centrifugal water pump is commonly used for agricultural purposes. It is widely used in agriculture to transport water from a water source, such as a river, dam, or bore, to a place of use or a storage facility, such as a water tank or an irrigation system, through pipes. The pump is required in the water filtration system to transports water from a water source, river, or stream to a water reservoir for filtering [68]. From the analytical calculations (**Appendix C**), a pump with a flow rate of 0.694 at the bottom level of the river will need to overcome a system height of 5.14 m. Based on this information, the power requirement for such a pump was determined to be 46.1kW.

### **3.8 Design Consideration for Combined Filtration System**

A family of four would consume about 10 litres of water each day, according to WHO [1]. As a result, assuming an extended family (a prevalent pattern in developing countries) and peak demand, the daily water requirement per person should be about 4 litres. Hence, looking at a household of 7 will require 40 litres of filtered water daily for drinking. However, they would also need some filtered water for domestic usage such as cooking. Hence, on average, this project considers the entire filtration process to filter about 50 litres of water in a day. Based on the flow rate of Potters for Peace (PFP) filters, 5.79 litres of water may be filtered in a 4-hour cycle with an average flow rate of 1.448L/hour. Using the assumption that each person drinks 250 ml (0.25l) of water every 1.5 hours, one person requires approximately 0.7 litres of water every 4 hours. This

means that out of 5.79 litres of filtered water, 4.9 litres will be consumed, leaving roughly 0.892 litres of water supply safety for each 4-hour filtration cycle (assuming a household of seven people). As a result of the initial calculations, the overall capacity of the entire filtration process, including all stages of filtration, is 6-7 litres. Provided the feed water tank is filled 3-4 times daily, this volume of water will be adequate for a household.

### **3.9 Operational Mechanism of the Combined System Works**

The operation of the filter system starts from the centrifugal pump (**Fig. 3.12**). The function of the pump is to draw unfiltered water from a storage tank at low pressure and transfer it to the reservoir tank (feed water). The feed storage tank houses the unfiltered water for the filtration process to begin. In the feed storage tank, water sensors are installed, which measure the water level in the tank to prevent the spillage of water during pumping. The system is set up to enhance flow under gravity. Plumbing materials such as silicon was used to ensure pipes works are adequately sealed to prevent leakage.

The beginning of filtration process starts with the ceramic filter. The ceramic filter deals with the absorption of particulates and dirt. The turbidity of the control sample water was compared with the filtrate to determine the efficacy of the ceramic filter. PDMS filter membrane was installed in-between filters to remove excess contaminants and sand particles that could have possibly dropped from the ceramic filter walls. The following filter in the system is the agricultural waste filter made from orange and banana peels. This filter mainly focuses on the removal of dissolved heavy metals. AC filter filter was used to improves heavy metals and particulate adsorption and improves the water's taste and odour [53]. The filtered water was stored in a tank for further characterization.

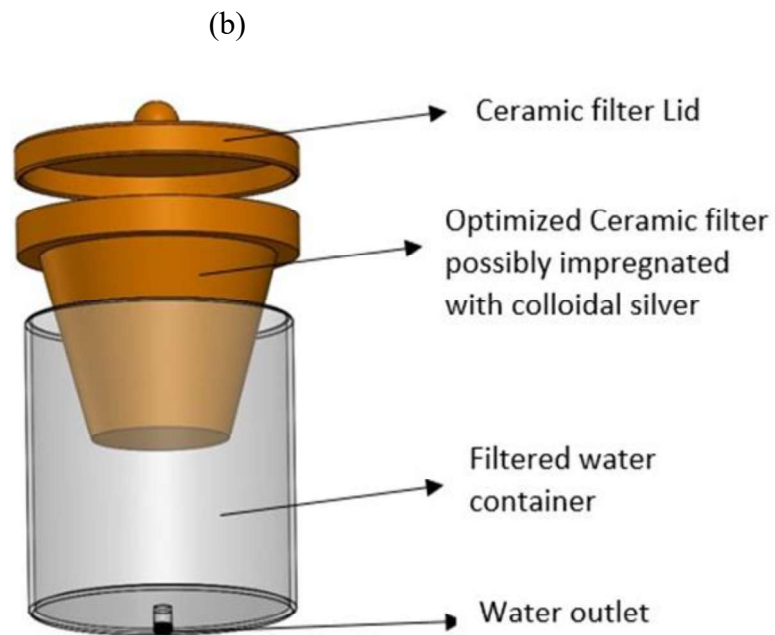
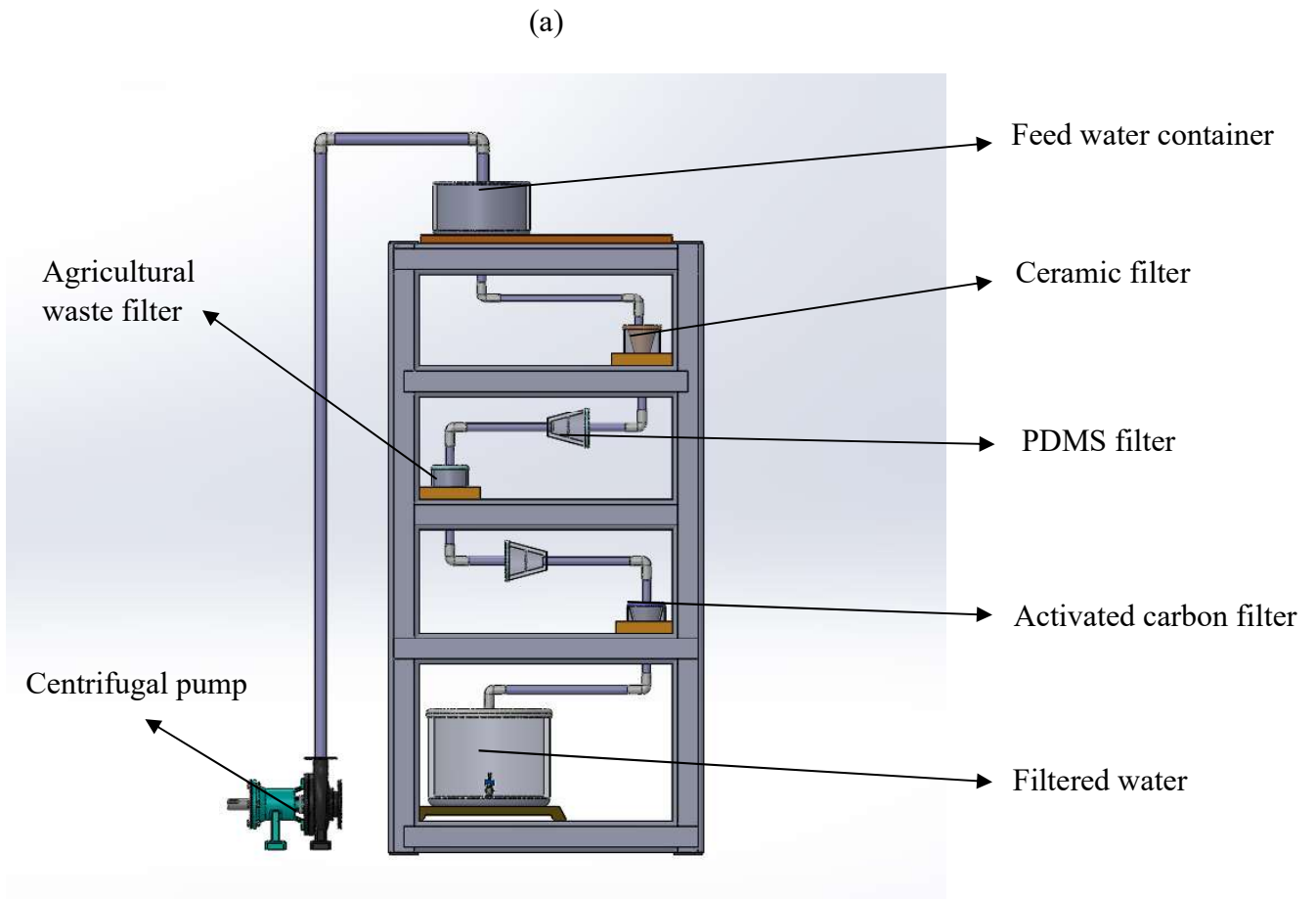


**Figure 3.12:** Proposed Final Design of the filtration system: Schematics of the Assembled Filters, and (b) Details of the Ceramic Section.

(c)

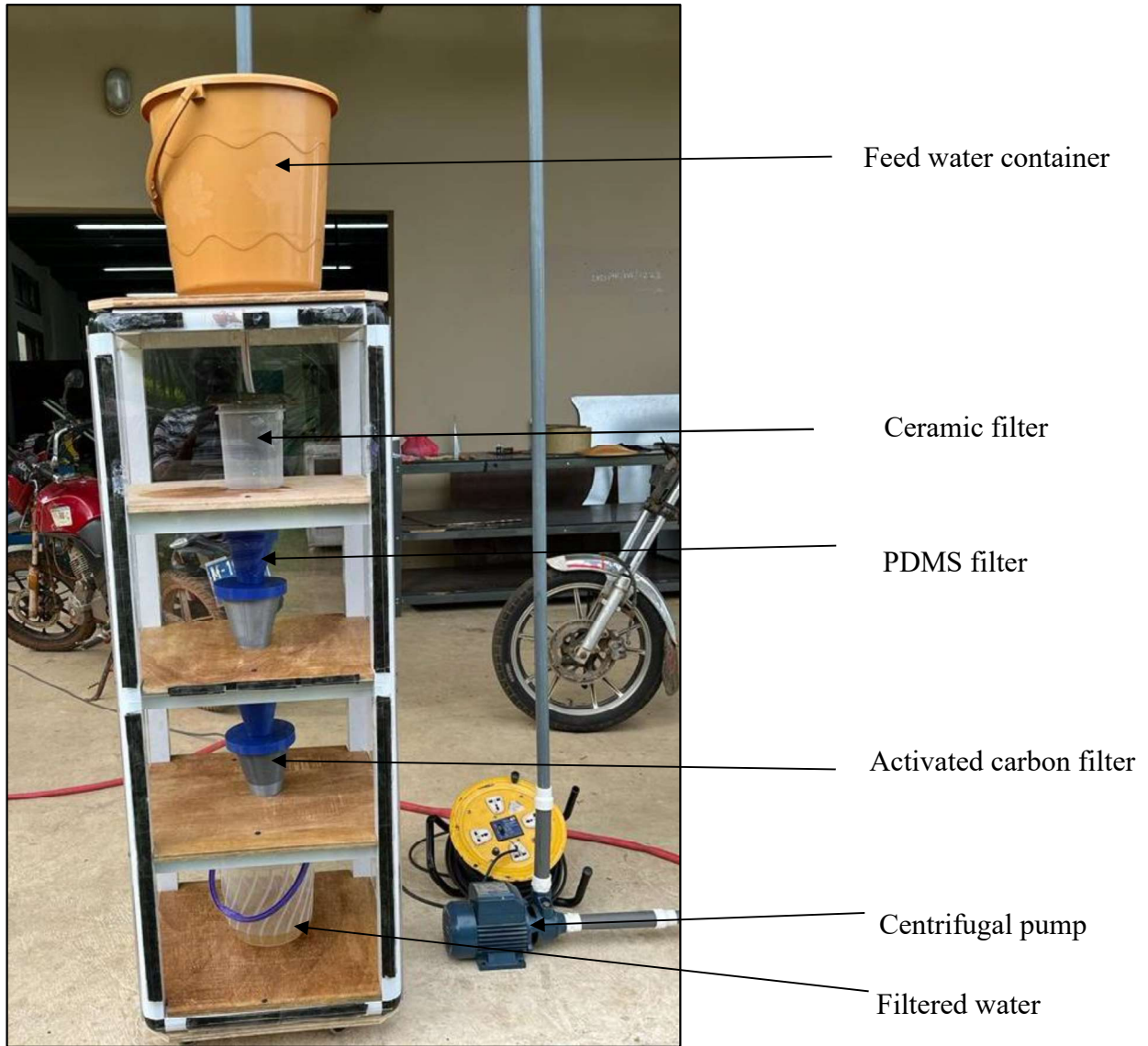


**Figure 3.13:** Proposed Final Design of the filtration system: Schematics of the Assembled Filters, (c) Fabricated System.

### 3.10 The Metallic and Support Structure

The feed water tank and the filtrate storage tank are the two main factors which may cause the steel structure to fail. Thus, the steel structure optimization study is concerned with how the structure can withstand the maximum weight (of all the filters and the two tanks) applied to it. Stress and strain analysis were used to determine the yield strength of the construction to determine the structural integrity. These figures were approximated based on research and assumptions, considering the various components of the filtration system.

**Table 3.1:** The estimated weights applied on the steel structure.

<b>Weight of feed water tank</b>	<b>1.3kN</b>
Weight of ceramic filter assembly	176.58 N (15 kg for ceramic filter, 3 kg for water)
Weight of agricultural waste filter	176.58 N (3 kg for water, 5 kg for filter)
Weight of activated carbon filter	176.58 N (3 kg for water, 5 kg for filter)
Weight of activated carbon filter	176.58 N (3 kg for water, 5 kg for filter)
Weight of PDMS filter	30N (1kg of PDMS filter and 2 kg of housing)
Weight for the filtrate storage tank	1.1 kN

### 3.10 Optimisations

#### 3.10.1 Ceramic Filter Impregnation with Colloidal Silver

The optimization study of the ceramic filter impregnated with colloidal silver deals with the change of dimensions, the apparent porosity, absorption, and flow rate of the ceramic filter. The percentage change in dimension of the ceramic filter impregnated with colloidal silver was determine using the expression.

$$P_d = \left| \frac{d_a - d_b}{d_b} \right| \times 100 \quad (3.1)$$

where  $P_d$  is the percentage change in the ceramic filter impregnated with colloidal silver,  $d_b$  is the diameter of the ceramic filter before colloidal silver impregnation,  $d_a$  is the diameter of the ceramic filter after impregnating with colloidal silver, and the apparent porosity and absorption were tested according to ASTM-C 373-88 standards, 2006.

$$p = 100 \left[ \frac{W_{saturated} - W_{dry}}{W_{saturated} - W_{underwater}} \right] \quad (3.2)$$

$$W_a = \frac{W_{saturated} - W_{dry}}{W_{dry}} \times 100 \quad (3.3)$$

where  $p$  is the apparent porosity,  $W_a$  is the water absorption,  $W_{saturated}$  is the weight of the specimen when saturated in water, and  $W_{dry}$  is the weight of the dry specimen and  $W_{underwater}$  is the weight of the sample underwater.

### 3.10.2 Heavy Metal Adsorption

Adsorption is a surface phenomenon whose extent is directly proportional to the specific surface area, so for a more powdered and porous solid, the greater the percentage of the adsorbate per unit weight. The fundamental equation governing the adsorption solid-liquid process is given by equation (3.4) [47].

$$q_t = \frac{(C_0 - C_t)V}{m} \quad (3.4)$$

where  $q_t$  (mg/g) is the amount of adsorbate per unit mass of adsorbent at a time,  $t$ .  $C_0$  (mg/L) and  $C_t$  (mg/L) are the initial and instantaneous time  $t$  concentration of adsorbate, respectively,  $V$  (L) is the volume of the solution, and  $m$  (g) is the mass of the adsorbent.

### 3.11 Flexural and Compressive Test on Ceramic Composites

For filtration application, the ceramic filter must support the load of the water, and it must do so without fracturing. Thus, it is important to characterize the filter compressive strength rather than its tensile strength. Moreover, according to [72], the Griffith theory predicts the compressive strength of ceramics to be 8 times larger than their tensile stresses due to local tensile stresses at the tip of pre-existing flaws. These flaws include cracks, voids, impurities, twinning, thermal expansion anisotropy and misalignment during testing [73]. As grain size appears to have a large effect on compressive strength, the clay was sieved by a fine mesh to obtain fine grain size distribution. Saw dust was also sieved to obtain minimum variation in the size to produce similar pore sizes when burnt out.

The compressive strength is simply the ratio of the applied load at failure to the cross-sectional area of the gauge-section.

$$\sigma = \frac{F}{A} \quad (3.5)$$



where  $F$  is the force at failure and  $A$  is the cross-sectional area of sample.

In this experiment, a three-point bend test was used to carry out flexural test. The span is assumed to be short since the span length is less than or equal to 16 times the thickness of the sample [69].

The specimen is set up with the Pasco testing machine as follows.

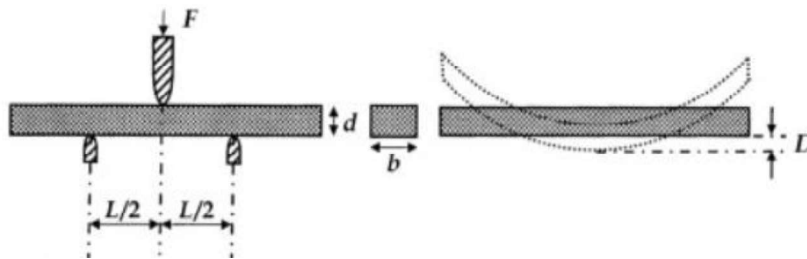


**Figure 3.14:** Three-point bend set-up for flexural modulus test.

where  $L$  is the support span length,  $F$  is the force at maximum deflection,  $d$  is the depth of the specimen,  $b$  is the width of specimen, and  $d$  is the maximum vertical deflection of specimen.

The load is applied at the center at a distance  $L/2$  equidistant from the lower support. The stress is given by:

$$\sigma_f = \frac{3FL}{2bd^3} \quad (3.6)$$

The strain is given by:

$$e_f = \frac{6dD}{L^2} \quad (3.7)$$

The flexural modulus which is given by the ratio of stress to strain is given by:

$$E_s = \frac{\text{Stress}}{\text{Strain}} = \frac{FL^3}{4bDd^3} \quad (3.8)$$

Below is an illustration of the flexural modulus test being carried out on the Pasco Machine.

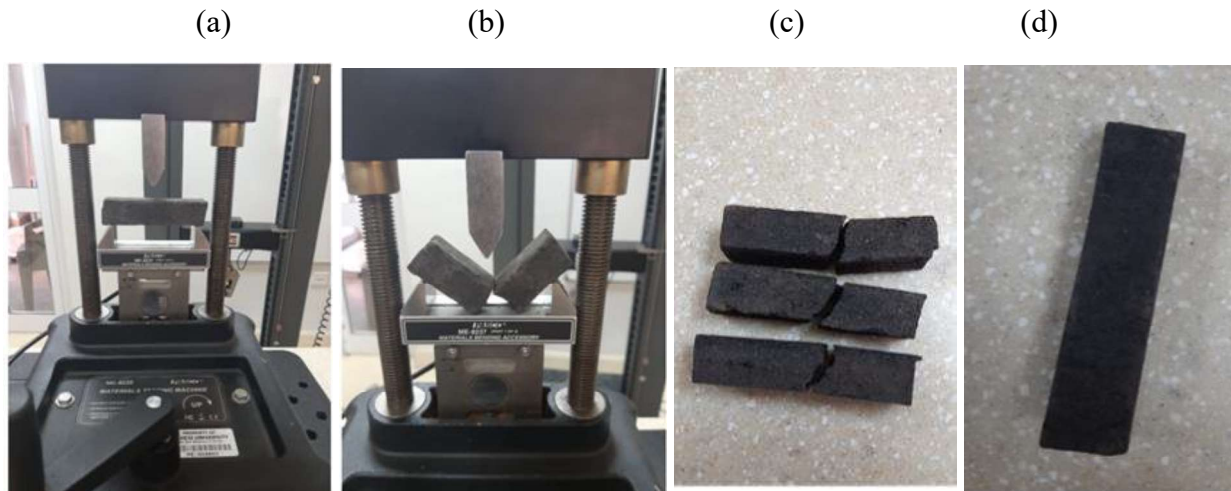


**Figure 3.15:** Flexural Testing: a) Pasco machine with sample, b) sample at the point of fracture, c) three samples showing failure occurring at 45 degrees, and d) rectangular sample for three-point bend test.

### 3.12 Tensile Testing of PDMS Specimens

The PDMS samples that were cast in the dogbone mould were taken to the Mechanical Engineering Laboratory for tensile strength tests. The two ratios that were used are 10:1 and 5:1 ratio. Four samples of each ratio were used to run the test. The Materials Testing System was used for the tensile strength testing. This machine utilized the PASCO Capstone software, which was used to record and graph the values obtained from the tests. Data obtained from PASCO software were exported for further analysis using OriginPro software (indicate the version).

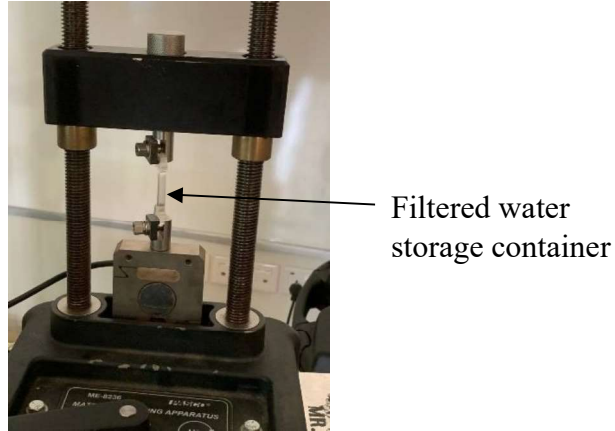


**Figure 3.16:** PDMS Sample under Tensile Test.

### 3.13 Porosity and Density

The porosity of the ceramic refers to the spaces that can be filled up by fluid. it is the proportion of the composition of a material that is filled by void spaces. Mathematically it is the ratio of the total pore volume to the bulk volume. It is given by:

$$\phi_t = \frac{\text{Total Pore Volume}}{\text{bulk Volume}} \quad (3.9)$$

where the bulk volume refers to the volume of the specimen as calculated using volume relations.

The specimen is rectangular in shape. Thus, their volume is given by:

$$\text{Bulk volume} = l \times b \times h \quad (3.10)$$

where l is the length, b is the breadth, and h is the height.

The total pore volume refers to the volume occupied by fluid in the spaces of the specimen.

$$V_p = \frac{W_{sat} - W_{dry}}{\rho_f} \quad (3.11)$$

Equation 3.11 calculates the volume of fluid occupied by pores.

Here, the specimen's weight is measured when dry ( $W_{dry}$ ). Then its saturated weight ( $W_{sat}$ ) is measured after being soaked in water or brine-the ratio of the weight difference between the saturated and dry samples to the fluid density.

In filtration application, the porosity is essential so that the pores within the ceramic filter can be characterized in terms of a percentage. This would give an idea of how much water can flow through.

### 3.14 Method of Determining Porosity and Density

The method of determining the density and porosity of the clay-sawdust samples can be accessed from **Appendix B2**.



**Figure 3.17:** Determination of Porosity and Density: a) set-up of samples in water, b) saturated samples, and c) saturated samples left on paper towel for droplets of water to dry before measurements.

## CHAPTER FOUR

### 4.0 Results and Analysis

#### 4.1 Mechanical analysis of the Structural Scaffold

Different loads were applied to the teak wood lying on the aluminium structure during the load analysis. According to the SolidWorks simulation (**Fig. 4.1a**), teak wood has a tensile strength of about 4.10 MPa and compressive strength of about 56 MPa. The teak wood did not yield because there were no critical places that were subjected to more significant stress than the yield strength of the material. The feed water tank has the most significant weight; as a result, its section is subjected to more stress than the other teak wood slabs. The wood supporting the feed water tank had the most displacement in terms of displacement and strain (**Fig. 4.1b-c**). Since the structure did not fail with any of the three tests, the aluminium structure is a good option to use as the scaffold of the filtration system.

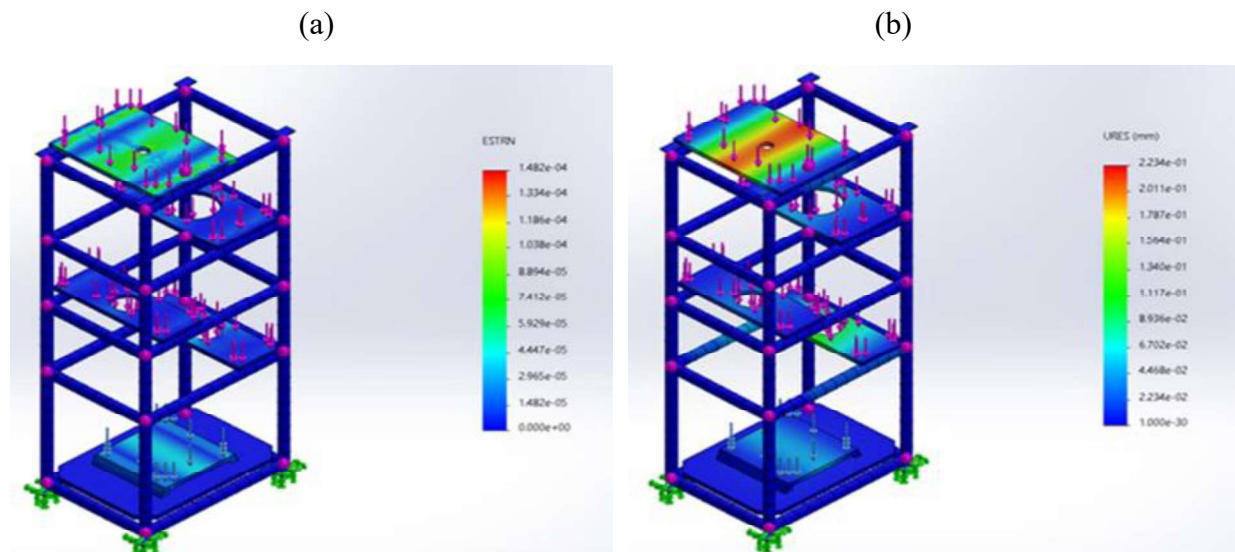


**Figure 4.1:** Load analysis simulation on the steel structure. (a) Displacement and (b) Strain.

(c)

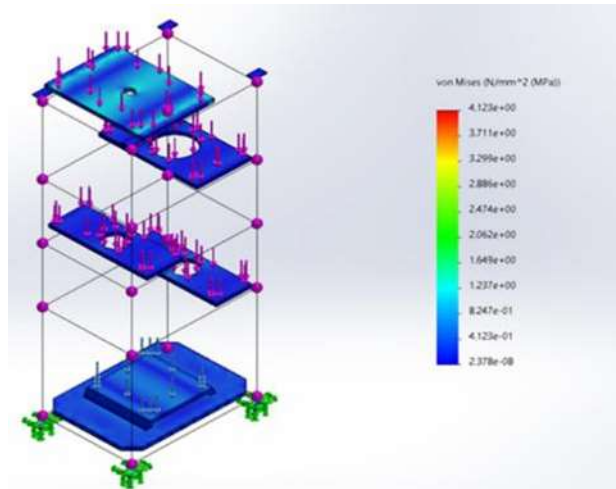


**Figure 4.2:** Load analysis simulation on the steel structure: (c) Stress Analysis.

## 4.2 Preliminary Water Quality Analysis

### 4.2.1 Measuring Flow Rate of Activated and Agricultural Waste Filter

In determining the flow rate, tap water was connected to ensure constant pressure and speed from the water source to obtain accurate results using the experimental set-up, as indicated in **Appendix A1. Table 4.1** represents the experimental data used to obtain the graphical representation in **Figure 4.2**. The experimental data are plotted to utilize origin, where the line of best fit is used after a scatter plot to determine the slope of the graph. From **Figure 4.2**, the slope of the plots which is  $\frac{Volume (mL)}{Time (s)}$  represents the flow rate. Hence, the flow rate of the activated carbon and agricultural waste filters were 3.005 mL/s which is 1.08 L/hr.

**Table 4.1:** Data Obtained from Experiment to measure flow rate of Activated carbon filter.

Cumulative Volume (mL)	Cumulative Time (s)
149	60
324	120
511.5	180
683.5	240
873.5	300
1048.5	360
1223.5	420
1413.5	480
1588.5	540
1770.5	600

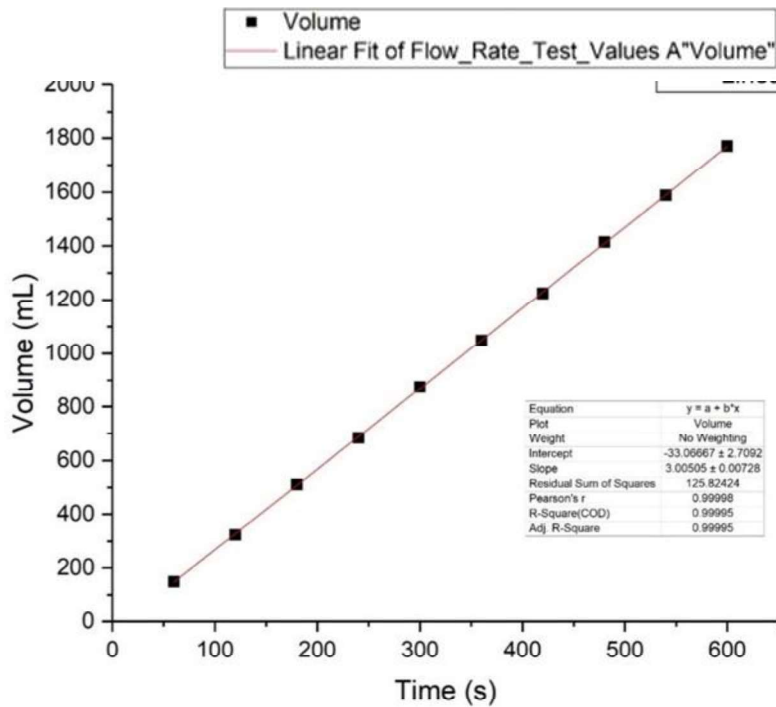


**Figure 4.3:** Graph to determine the flow rate of the agricultural waste and activated carbon filter.

#### 4.1.2 Water Quality Analysis with a Commercial Granular Activated Carbon

This was an initial control test done by utilizing the commercial granular activated carbon to filter three water samples (**Appendix A2**). For each quality analysis test, data points were collected using LoggerPro in under 120 seconds, yielding 60 and 120 data points, respectively. The standard deviations, mean, and median values were calculated, and the measurement that best fit the situation was chosen for analysis.

**Figure 4.3** shows that the turbidities of the various water samples were significantly reduced, particularly for water samples from Nana Mall and Abandza rivers, which had turbidities of 670 NTU at the start. The Nana Mall River water was less turbid after filtration than before, as indicated in **Figure 4.3c**. However, despite remaining within the acceptable WHO drinking water standard, conductivity was found to have increased; this increase in conductivity could be attributed to the fact that removing total organic carbon from contaminated water using adsorption on activated carbon frees the ions to move. Thus, causing the conductivity to increase after filtration with activated carbon. On the other hand, the pH was maintained, although with a minor variation. They do; however, all meet the WHO standard for drinking water. Although the turbidity of the water appeared to have improved, it still did not reach the WHO requirement; therefore, a larger volume of granular activated carbon is necessary for effective performance and safe drinking water.



**Table 4.2:** Water Quality Test for Control Test.

Water Sample	Turbidity (NTU)		pH		Conductivity( $\mu\text{s}/\text{cm}$ )	
	<u>Before</u>	<u>After</u>	<u>Before</u>	<u>After</u>	<u>Before</u>	<u>After</u>
River Densu	25.58	5.92	6.57	6.98	253.9	261.5
Nana Mall	670	65.72	6.25	6.73	239.4	253.0
Abandza	670	356.9	7.02	6.95	78.39	261.9
WHO standard for drinking water	<5		6.5-8.5		<400	

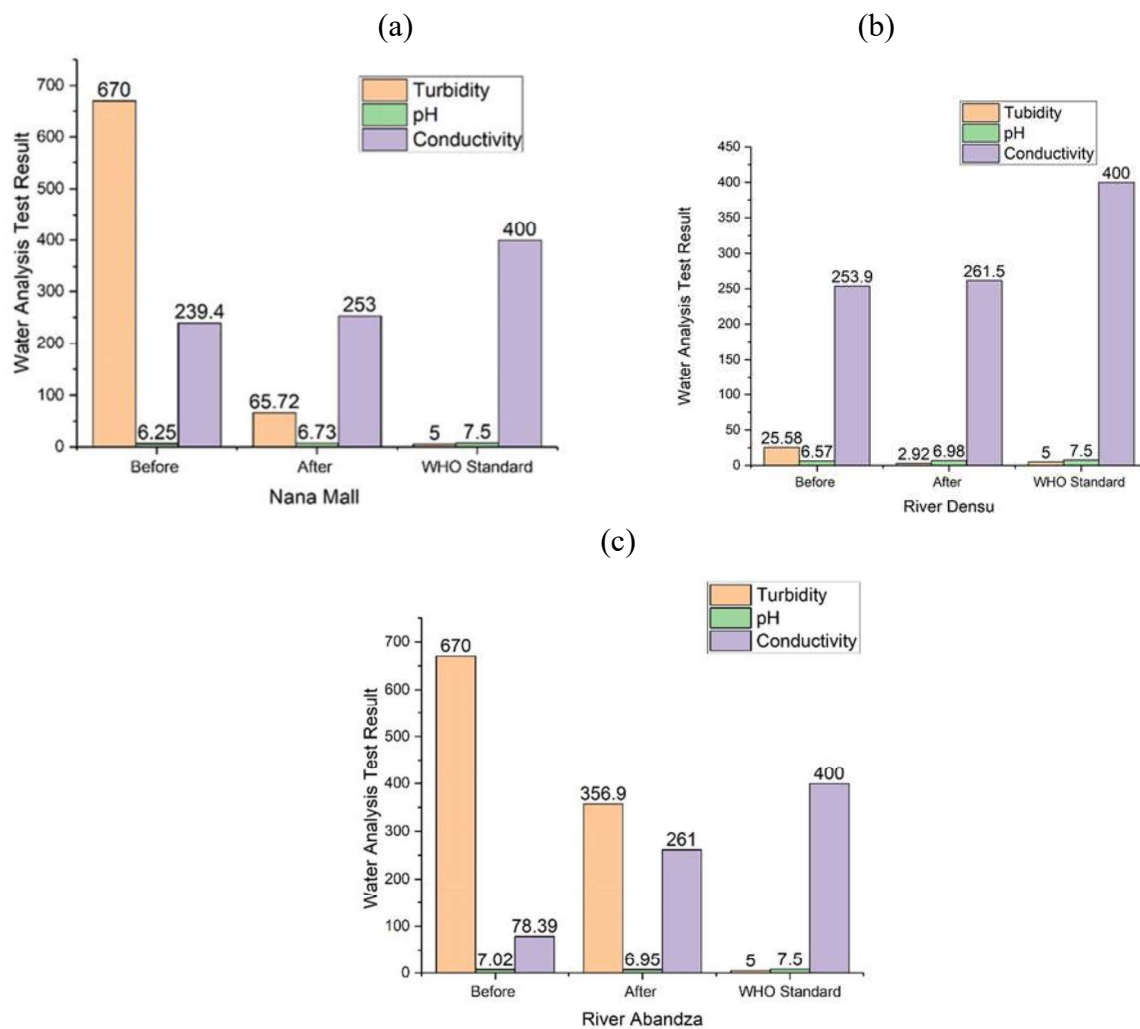


**Figure 4.4:** A graph showing the turbidity, pH and conductivity of the three water samples before and after filtration with granular activated carbon, compared with the WHO standard: (a) River Densu, (b) Nana Mall River, and (c) River Abandza.

## 4.2 Testing the Effectiveness of the Locally Made Activated Carbon

A similar setup in **Appendix A1** was used to perform the locally made activated carbon test. The result obtained for the Nana mall water sample is shown in **Table 4.3**.

**Table 4.3:** Water Quality Analysis Results for Locally Made Activated Carbon.

	Turbidity (NTU)	pH	Conductivity ( $\mu\text{s}/\text{cm}$ )
Water sample before filtration	670	6.25	239.4
Water Sample after filtration	305.9	6.53	242.1

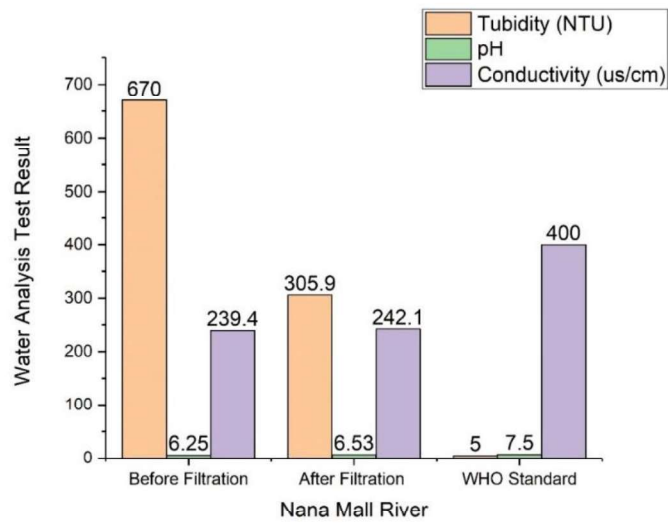


**Figure 4.5:** A graph showing the turbidity, pH and conductivity of Nana Mall Water sample before and after filtration with locally activated carbon, compared with the WHO standard.

From **Figure 4.4**, the findings of the locally created activated carbon were like those of the commercial granular activated carbon; however, the turbidity of the water was reduced by 54.3% with the locally made activated carbon. On the other hand, there was a 90.25% reduction in

turbidity when commercial activated carbon was used. As a result, locally activated carbon reduces turbidity, but it is not as effective as commercial activated carbon. Hence, factors contributing to this deficiency for the locally generated activated carbon, such as the preparation method, must be revised to ensure optimization and the best turbidity effect.

### 4.3 Apparent Porosity and Density of Porous Clay Filters

The calculated data on porosity and density of the prepared composites of clay-based composites are represented (**Figure 4.5**).

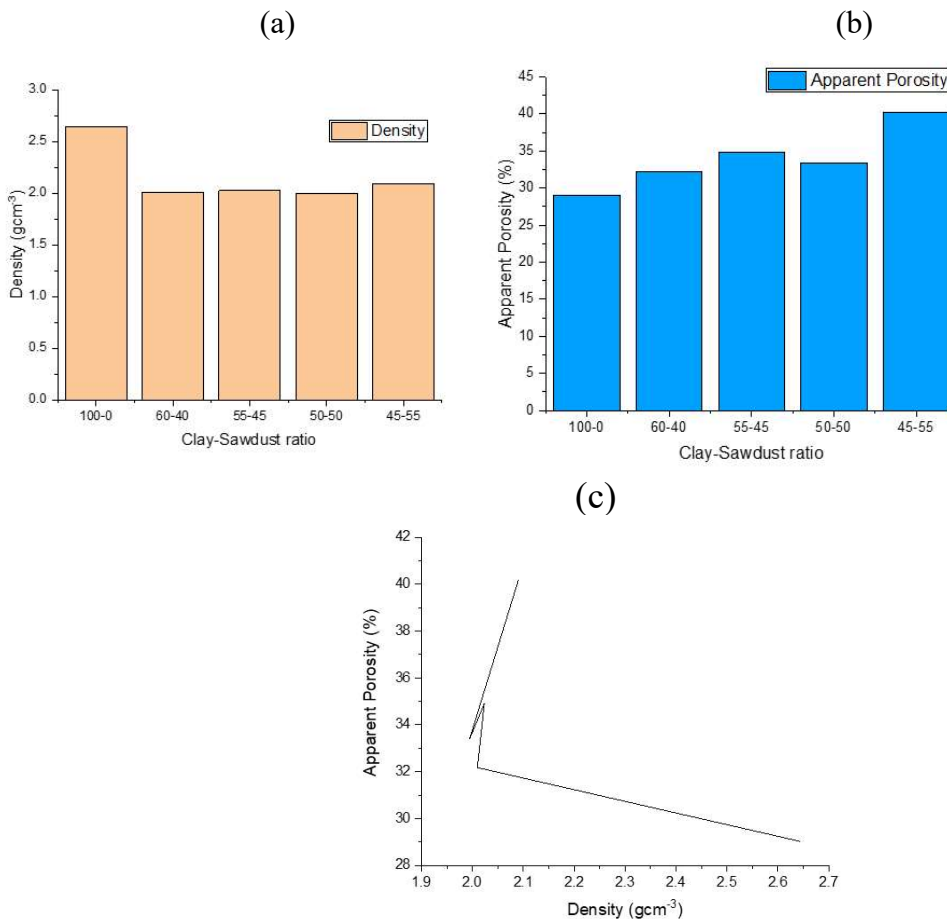


**Figure 4.6:** A plot showing the density and apparent porosity (%) of the different clay-sawdust ratios: (a) Density, (b) Apparent Porosity, and (c) Relationship between Density and Apparent Porosity of the Samples.

The results from the apparent porosity and density (**Fig. 4.5a-b**) suggest that all the samples are two times denser than water. The apparent porosity values are in line with the assertion that the sample with more sawdust is more porous. Thus, density and porosity of the ceramic filter are inversely related [74]. Hence the clay-sawdust ratio of 45-55, with the greatest sawdust percentage of 55%, was most porous with a porosity value of 40.18%. Ideally, the density and porosity of the samples are supposed to be inversely proportional. However, from the apparent porosity and density plots (**Fig. 4.5c**), only the extreme cases of the clay-sawdust ratios obey this rule. With this, the sample with the least amount of sawdust (100-0) which implies 100% clay and 0% sawdust, was the densest and the least porous. Also, the 45-55% clay sawdust ratio has a significantly larger porosity than all the other ratios. Its density, however, is not substantially smaller than the rest, as the theory suggests. The ratios: 60-40, 50-50, and 55-45 have very close density values, even though their porosities are a little further apart. This may be because the difference in the sawdust ratio is 5% for the three ratios.

#### **4.4 Results from Filtration with Ceramic Water Filter**

The preliminary water analysis presents the values of turbidity, conductivity, and pH measured (**Fig.4.6a-d**) using the Vernier turbidity, conductivity, and PH sensors and the LoggerPro application. These values represent the actual values from raw water samples taken from galamsey sites, namely Abandza river, Nana Mall River, and River Densu. The most turbid of the three water samples were used for pre and post-filtration analysis with the same measuring apparatus and software. The optimum filter was 45-55 (clay: sawdust ratio). It produced water with less turbidity with a percent reduction of 98.67%NTU from the original water sample.

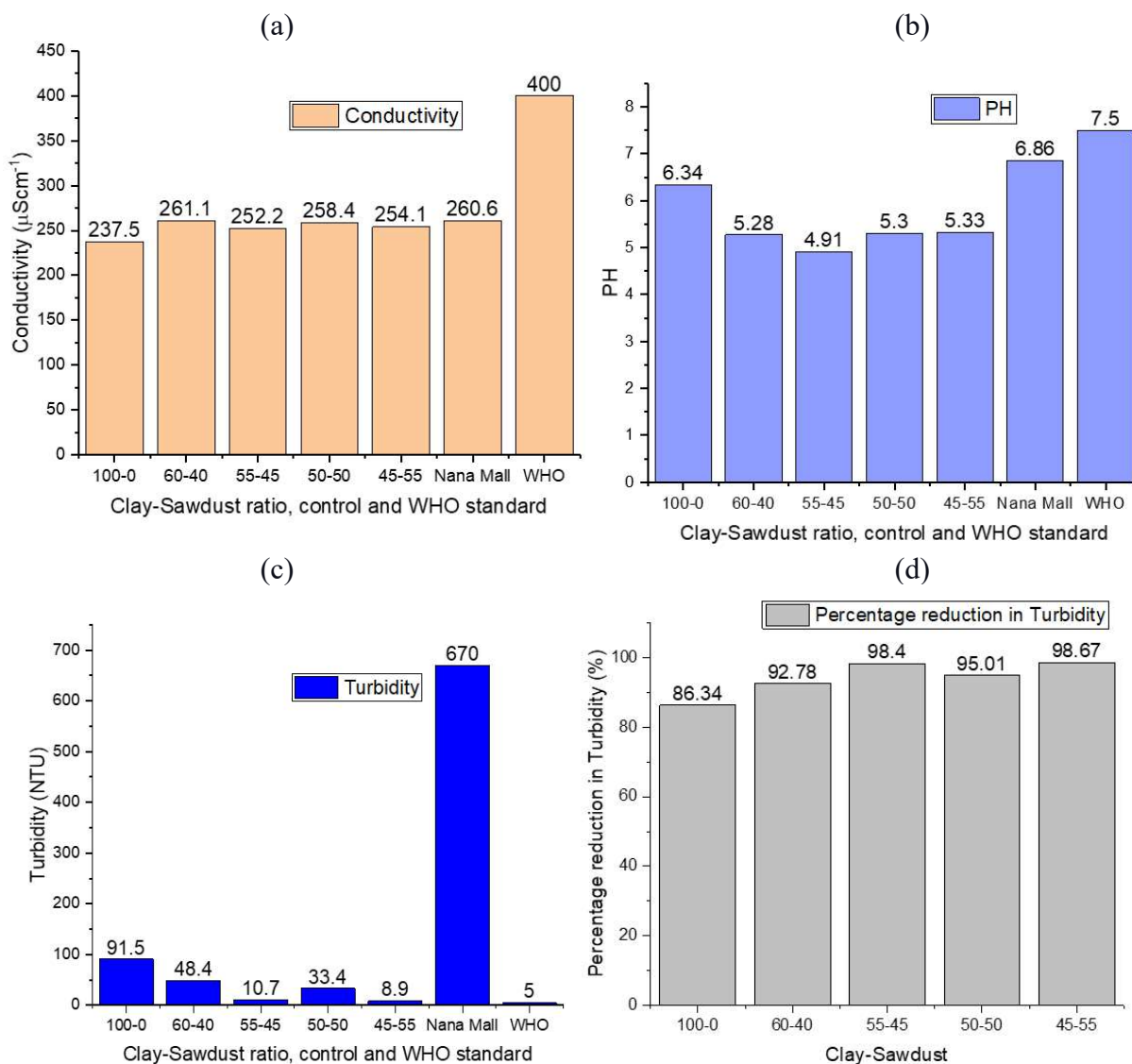


**Figure 4.7:** Nana Mall Water Filtration with Ceramic Filter from the Different Clay-Sawdust Ratios: (a) Conductivities of water filtered, (b), pH of Water Filtered, (c) Turbidity (NTU), and (d) the Turbidity of Water Filtered from the Different Clay-Sawdust Ratios.

#### 4.5 FTIR Analysis of the Herbs

Fourier Transform Infrared (FTIR) analysis involves subjecting a sample to infrared radiation, in which the radiation causes atomic vibration of molecules in the sample.

#### 4.6 X-Ray Fluorescence (XRF) Analysis of the Quenchant

X-ray Fluorescence (XRF) is used to identify the elements and oxides in a sample by recording the characteristic x-ray fluorescence produced by the sample. Each element and oxide in the sample produces a unique “glow” when excited by primary x-ray radiation. This unique characteristic glow is used to identify specific elements and oxides present in the unknown sample. The XRF analysis of Birsana and Nyen-nyol, identified elements and oxides can be accessed from **Table J2 and J3 of Appendix J.**

The most common oxides in both herbs are SiO<sub>2</sub> (41% in Birsana and 21.4% in Nyen-nyol), Calcium Oxide (18% in Birsana and 63.1% in Nyen-nyol). Magnesium Oxide is high in Birsana (13.2%) as well as Potassium Oxide (12.6%). From research, nano-SiO<sub>2</sub> is added in colloidal or powder form to increase the compressive strength and elastic modulus of building concretes [75, 76,77]. Thus, the composition of Birsana and Nyen-nyol suggests that it could improve the mechanical properties when used infused in ceramics by quenching.

#### 4.7 Tensile Strength of PDMS Samples

From **Table 4.4**, the samples with a PDMS: Crosslinker ratio of 5:1 needed a greater force and to break the samples. The sample experiences larger strain which is typical of PDMS. This is interpreted as the 5:1 sample have a greater ultimate tensile strength to the 10:1 sample. Going forward, the 5:1 ratio was the favourable ratio to use. However, to gain accurate values for the ultimate tensile strength for both ratios, the data gained from the PASCO Capstone software was transferred to Origin Software (2017 version) and the Stress-Strain graphs were obtained.

**Table 4.4:** Peak Loads and Extension Displaced by PDMS-Matrixes.

Ratio	Position	Force	Position	Force	Position	Force	Position	Force
	#1 (m)	#1 (N)	#2 (m)	#2 (N)	#3 (m)	#3 (N)	#4 (m)	#4 (N)
5:1	0.05332	21	0.05406	20	0.0527	16	0.0527	16
10:1	0.02308	12	0.02229	11	0.02499	13	0.02744	14

An example of a Stress-Strain graph (Fig. 4.7) that was obtained is shown. Table 4.5 shows the ultimate tensile strength values obtained from the stress strain curve.

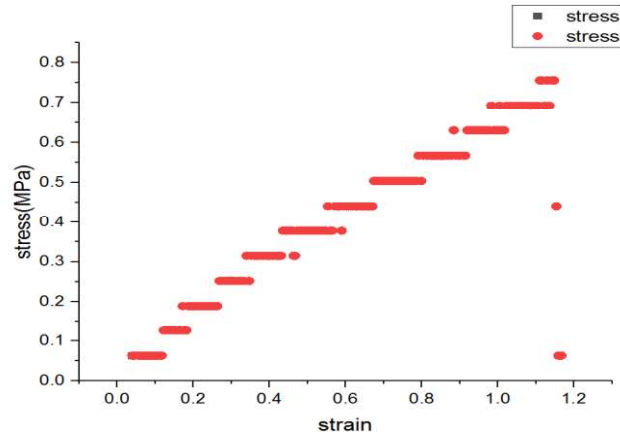


**Figure 4.8:** Stress-strain curve for a 5:1 PDMS sample.

#### 4.7.1 Statistical analysis

(Appendix II) is done to ensure that a fair comparison can be made between the two ratios. The distribution is found to be normal, and an independent t-test with unequal variance is run on young's moduli of the ratios. The p-values obtained is less than 0.05, indicating a significant difference in the test means. Thus, the null hypothesis was rejected. The variance between the two groups is unequal and a fair comparison can be made.

**Table 4.5:** Ultimate Tensile Strength values obtained from Stress-Strain curves.

Ratio	Run 1 (MPa)	Run 2 (MPa)	Run 3 (MPa)	Run 4 (MPa)	Average (MPa)
5:1	1.31024625	1.25140108	1.18627229	1.30752901	<b>1.26386</b>
10:1	0.75737	0.7547726	0.821030286	0.87857345	<b>0.80294</b>

From the results gained from the Stress-Strain curves, the 5:1 ratio sample has greater ultimate tensile strength average of 1.264 MPa, thus, this ratio was used in the preparation of the PDMS membrane.

#### 4.8 Effect of thickness of PDMS Filter

##### 4.8.1 Flow Rate

After the sugar cubes were leached from the cured PDMS membrane, foams were formed, taking the shape of the sugar cubes. A test was then done to investigate the effect of the thickness of the filter on the filtration process.

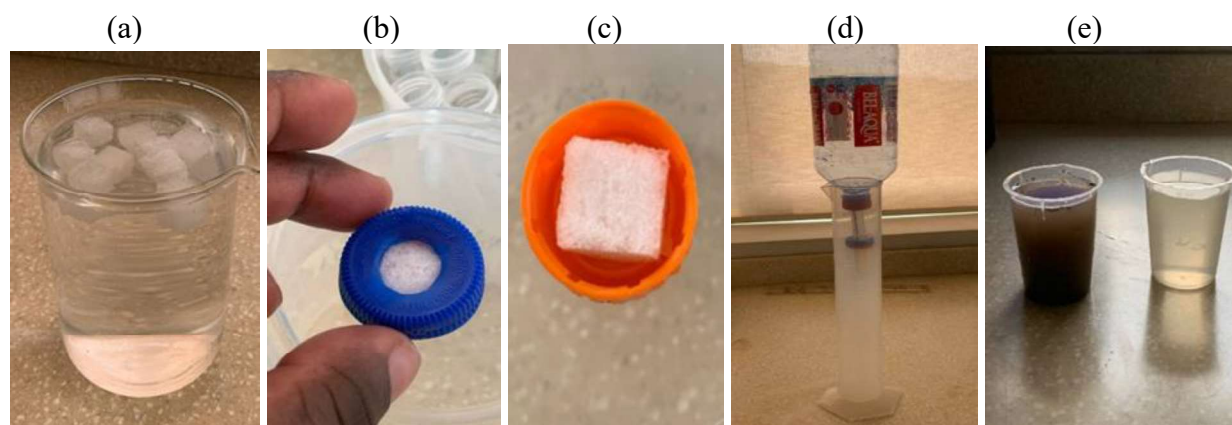


**Figure 4.9:** (a) leached sugar cubes, (b, c) experimental set up of filtration process (d) foam placed in bottle cover (e) unfiltered and filtered water.



The thickness of the PDMS foam that were used for the experiment are 0.5 cm and 1 cm. This is to analyse the effect of the film thickness of the membrane on the flow rate of the filter. The slope of both graphs was obtained from the Origin software. The slope represents the flow rate of the foams. For the 0.5 cm thickness foam, the flow rate was found to be 0.330 L/Hr whereas that of the 1 cm thickness foam was found to be 0.194 L/Hr.

Thus, moving forward, a filter membrane of a smaller thickness is seen to increase the flow rate of the filter. However, a thick film/membrane ensures low turbidity.

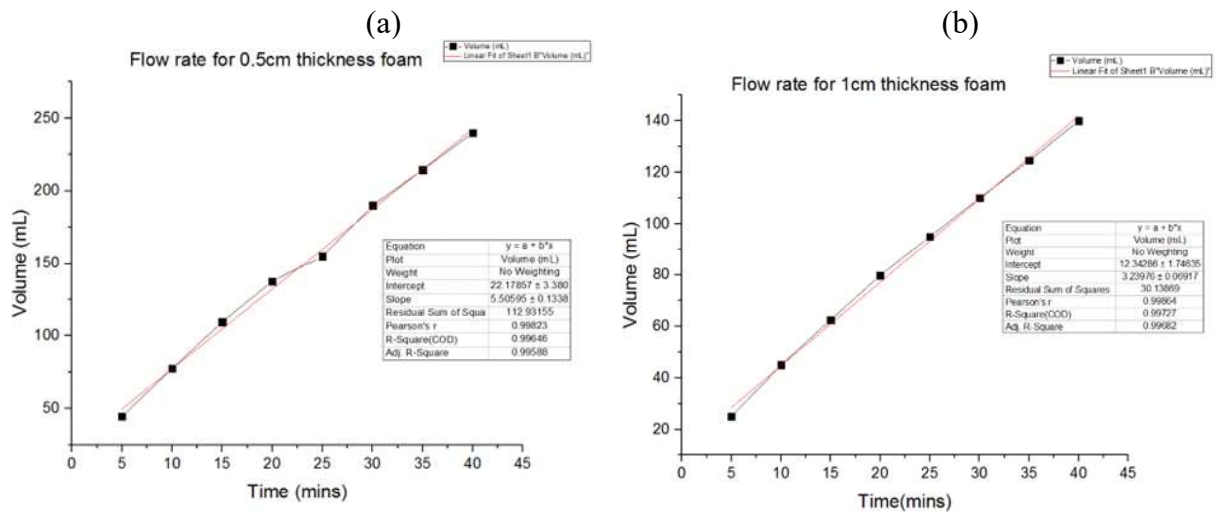


**Figure 4.10:** (a) Flow rate graph for 0.5 cm thickness (b) Flow rate graph for 1 cm thickness.

#### 4.7.2 Water Quality Analysis using PDMS Filter Membrane

The effect of the thickness of the filter membrane on the pH, conductivity, and turbidity was analyzed (Fig. 4.10). From the results obtained from the Origin Software, for a membrane thickness of 0.5 cm, it has great effect on the turbidity, and pH. However, it does not have much effect on the conductivity, the same can be said for the membrane of 1 cm film thickness.

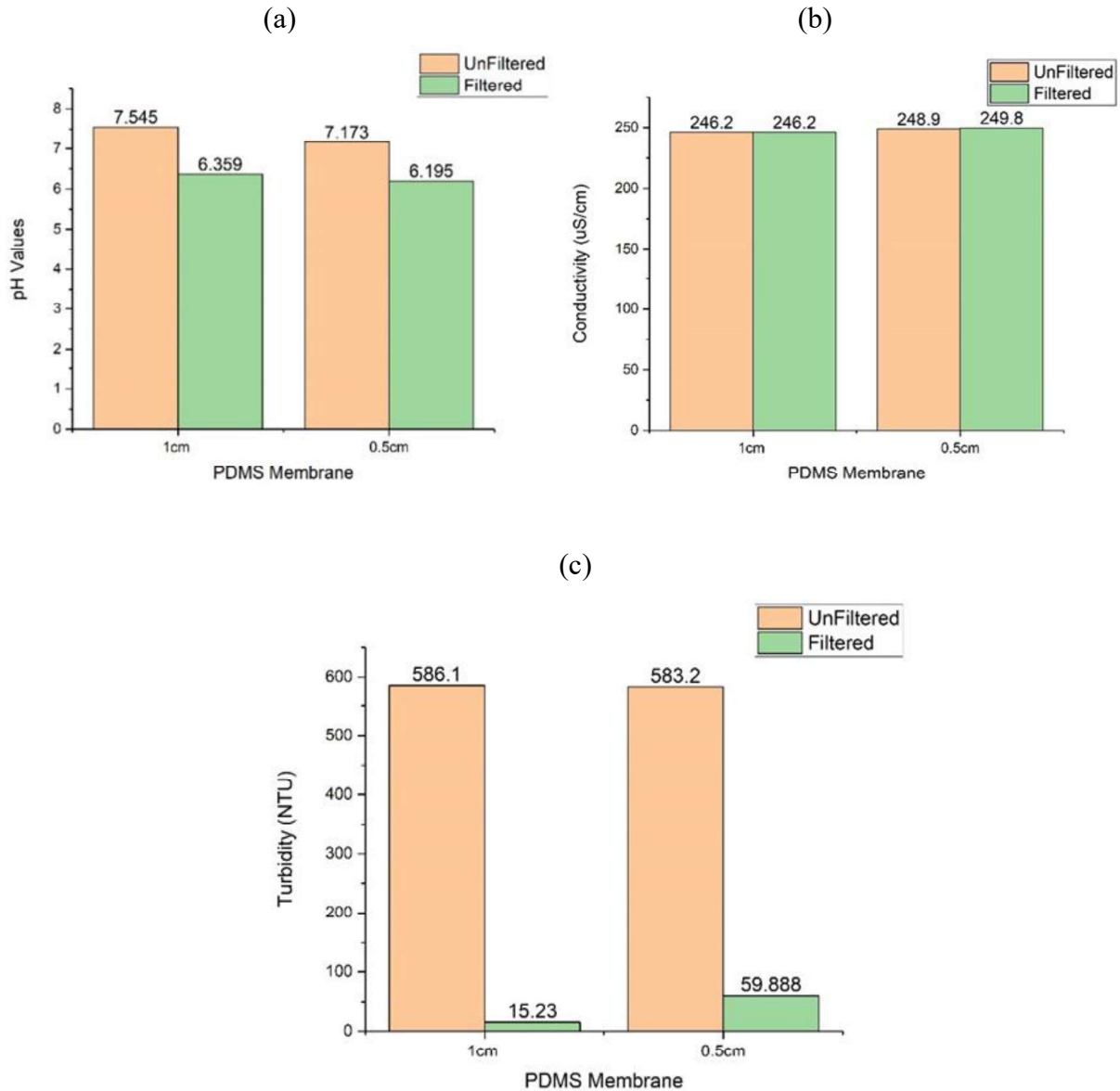


**Figure 4.11:** Effect of PDMS Membrane Film Thickness on Water Quality: (a) pH of the water (b) conductivity (c) Turbidity.

#### 4.8 Flow Rate of the PDMS Filter

The figure below (**Fig. 4.11a**) shows the values recorded on the volume of water collected per second. The slope of the graph represents the flow rate of the filter. The slope of the graph is obtained to be 5.4 L/hr. This flow rate is adequate to support the overall system toward providing

water for households. The three water samples, River Densu, Nana Mall River, and Abandza River were used for the tests. The pH, conductivity, and turbidity for the water samples and the filtrates collected are tested and presented (Figs. 4.11b-d).

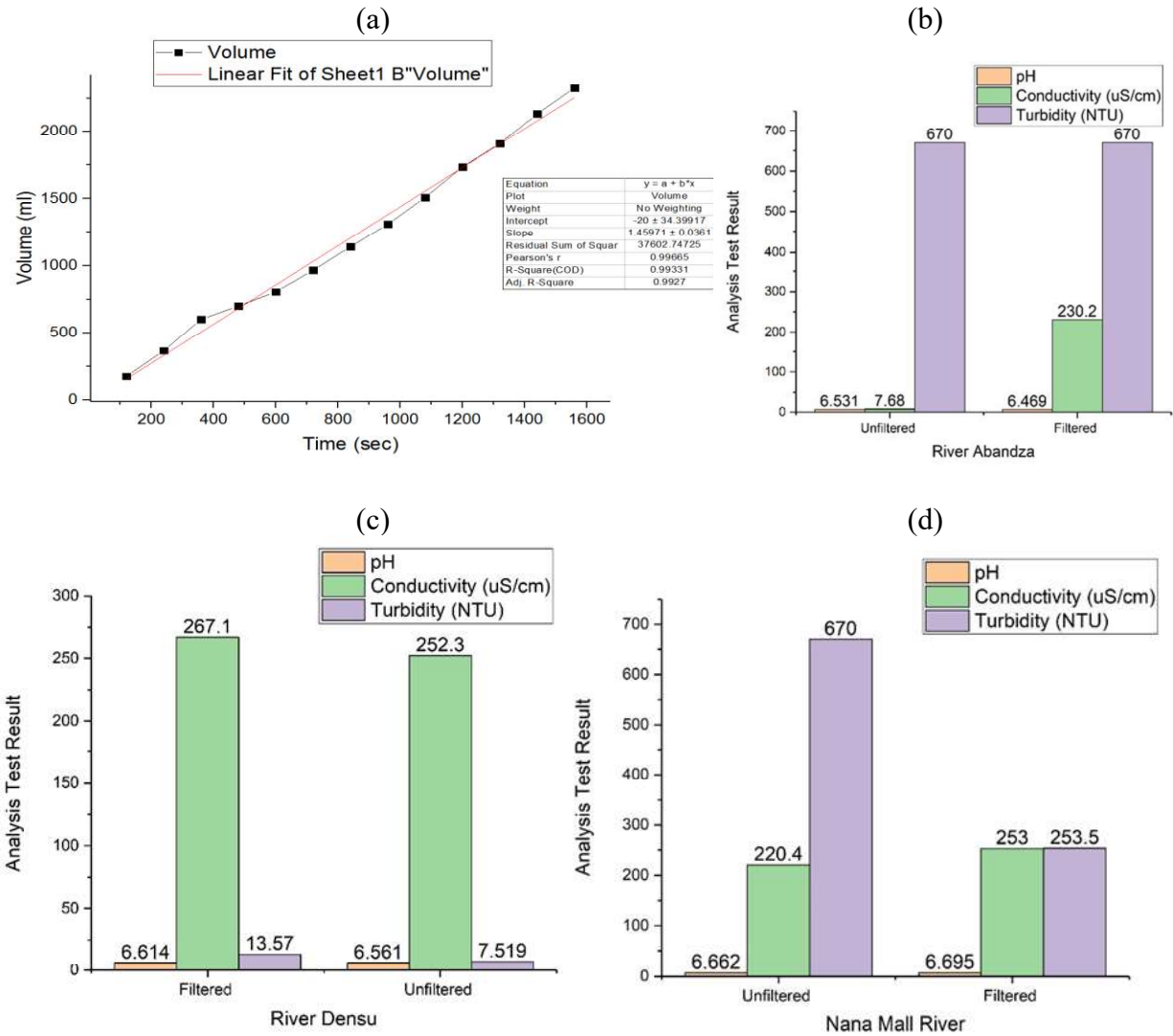


**Figure 4.12:** Flow Rate and Water Quality Obtain from PDMS Membrane Film: (a) Volume of Water Collected versus Time, (b) Data from River Abandza Water, (c) Data from River Densu, and (d) Data from Nana Mall River.

From the results obtained from the tests (**Fig. 4.11b-d**), River Densu sample performed the best from the filtrate that was collected. The pH, conductivity, and turbidity reduced to a preferable level, showing that the PDMS membrane served its purpose. However, for other water samples, even though there were some improvements, the turbidity remained the same for the Abandza River water sample.

#### 4.9 Water Quality Analysis of Final Filtrate

##### 4.9.1 pH, Turbidity and Conductivity Analysis

From the result in **Figure 4.12**, it was observed that the pH and conductivity of the filtrate water stayed within the WHO standard for drinking water. However, although the turbidity of the water samples was reduced by 83.73%, the final value obtained was above that of the WHO standard for drinking. However, this could still serve other domestic purposes such as washing, watering, etc.

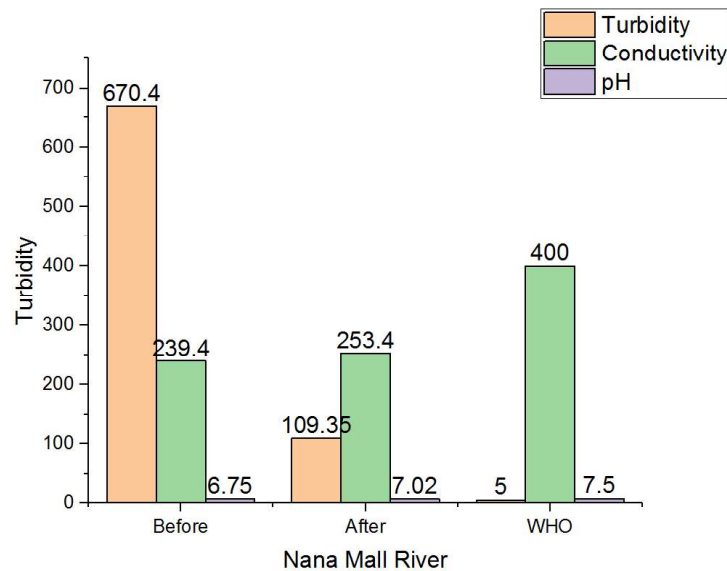


**Figure 4.13:** Graph showing turbidity, conductivity, and pH of the filtrate water from the entire filtration system.

#### 4.9.2 Heavy Metal Concentration Analysis

The data (**Table 4.6**) indicates the concentrations of heavy metals in sample water. The water sample collected already contained low levels of heavy metals. Hence, the effect of heavy metal removal was not significant, except for the case of zinc. These levels are acceptable within the WHO standards for drinking water.

**Table 4.6:** Heavy Metal Concentration in Nana Mall Before and After Filtration.

<b>(mg/l)</b>	<b>Copper</b>	<b>Zinc</b>	<b>Lead</b>	<b>Arsenic</b>	<b>Cadmium</b>
<b>Filtered</b>	<0.010	0.033	<0.005	<0.001	<0.002
<b>Unfiltered</b>	<0.010	0.180	<0.005	<0.001	<0.002
<b>WHO Guideline</b>	2.0	2.0	0.001		0.005

## CHAPTER FIVE

### 5.0 Conclusions and Recommendations

#### 5.1 Conclusions

This project entails designing and building water filtration systems for particulate adsorption and heavy metal removal. It comprised of an assembled ceramic filter, PDMS filter, an activated carbon filter, and orange peels filter.

The ceramic water filter was made as a point-of-use filtration system to filter water for use in places with no access to a centralized water supply system. It was made by combining clay and sawdust (C-S) in ratios of 100-0, 60-40, 50-50, 55-45, and 45-55 by volume. Polluted water from galamsey sites were collected and analyzed for turbidity, conductivity, and PH before and after filtration with the five filter configurations. The percentage decrease in turbidity of the Nana Mall River water samples when filtered by the ceramic water filter ranged from 86.34% (lowest) to 98.67%(highest). The filter configuration of 45% clay and 55% sawdust was chosen as the optimum filter since it produced a water sample with the most significant reduction in turbidity. The data on porosity and tortuosity supports fluid dynamics, especially in particulate adsorption and water purification.

Activated carbon was obtained from coconut coir fibers for effective particulate adsorption. Because of its high adsorption capacity, activated carbon is highly recommended for water filtering systems. Thus, the produced AC reduced water turbidity by 54.3 per cent compared to a commercial granular activated carbon, which reduced turbidity by 90.25% indicating that the activation temperature should be increased beyond the current 300°C. However, the surface area and porosity of different activated carbons vary. In addition, an attempt has been made in this project to focus on recent developments in the use of orange peels for heavy metal removal.

The PDMS membrane filter helped improve the filtration of each of the filter's sections. When Polydimethyl-siloxane was cured and cast on granulated sugar particles or granulated salt particles/crystals, it takes the shape of it, forming a foamy structure. This is done to ensure there are pores that are small enough for water to pass through it but then trap contaminants in the water. Activated carbon was added to the PDMS-based membrane (matrix) to ensure the membrane can improve the turbidity of the filtrate.

The results show the possibility to develop an in-house water filtration system to solve the numerous water challenges in the country and beyond.

## **5.2 Limitations**

The project was limited by the number of processes involved in making the ceramic filter samples and the filter itself. Processes such as crushing, sieving, and soft working for consecutive days and a unique drying process made the preparation of the samples and filters tedious and labour intensive. Also, the lack of an electric furnace with temperature control was also perhaps the most significant limitation of this project. The clay-sawdust samples and filter needed to be fired at temperatures (around 900 to 1000 degrees Celsius), which were impossible to achieve and control with the improvised furnace on hand. This could explain why the filters absorb almost all the water poured into them while filtering only a small amount.

According to [74], the combination of a manufacturing process for the ceramic filter achieves greater compaction, such as mechanical press forming and slip casting, and a furnace to bake the ceramic filter produced filters with porosity within the range of 53-86. Because the filter is ceramic, the level of compaction plays a significant role in the strength of the final product. It

would determine if the filter would crack or it would stand the test of time. The filter was created using a hand-held mechanical press mould, and the final shape was formed by hand. This was accomplished by first forming the primary shape with the press, then scooping the clay-sawdust paste and forming the required shape by hand. Consistency in the level of compaction of the ceramic filter was not achieved in this manner.

Finally, due to the high cost of the elastomer and the curing agent used in the preparation of PDMS, and their scarcity in the country caused one to limit experimental samples.

### **5.3 Recommendations and/or Future Works**

The MTS Universal testing machine will determine the samples' flexural modulus and compressive strength for more accurate results. The Pasco machine was available for testing at the time. However, manually controlling the loading rate was problematic. Because of the nature of the sample (ceramic), it does not undergo elastic deformation, and an abruptly applied force causes the sample to fail in the same manner, transforming the test from a three-point bend test to an unfavourable impact test.

To produce the optimal concentration of the quenchant solution, the amount of herbal quenchants (Birsana and Nyen-nyol) must be measured. The optimal amount is determined by experimenting with different concentrations on baked samples and testing the mechanical properties. The corresponding concentration and number of herbs used would be considered optimal for the samples to produce the desired mechanical properties. If an electric furnace with a controlled temperature is used, the filter will have optimal porosity, and the flow rates will be quantifiable.



The carbonization and activation stages are critical in the preparation of activated carbon. The coconut coir fibre is carbonized at 900 degrees Celsius for 30 minutes in a furnace in a nitrogen atmosphere. The adsorption effectiveness varies depending on the carbonization and activation process used. Thus, future work could utilize the various carbonization and activated processes to obtain the optimum approach that results in approximately 90% adsorption efficiency. This will allow for more efficient adsorption, making polluted water safer to drink.

Another recommendation for the future is to investigate the influence of colloidal silver on bacterial deactivation. Pathogens and turbidity are removed from drinking water using colloidal silver. It acts on the metabolism of the bacteria; the silver binds to the bacterium's cell membrane, preventing cell respiration and killing the bacterium. They can be built with locally sourced materials, assisting in the growth of local commerce. Silver rods for electrodes, batteries, distilled water, and beakers can all be used to make colloidal silver at home. As a result, this could be investigated in future works.

## References

- [1] E. Yeleliere, S. J. Cobbina and A. B. Duwiejuah, "Review of Ghana's water resources: the quality and management with particular focus on freshwater resources," *Applied Water Science*, vol. 8(93), 2018.
- [2] S. Sharma and A. Bhattacharya, "Drinking water contamination and treatment techniques," *Applied Water Science (2016)* pp. 1043 – 1067.
- [3] A. E. Duncan, J. Oti and M. E. Potakey, "Impacts of Human Activities on the Quality of River Water: A Case Study of River Densu in Nsawam Adoagyiri of the Akwapim South District, Eastern Region of Ghana," *Open Access Library Journal*, Vol. 6 (2019) p. e5785.
- [4] World Health Organisation, 2019, "Drinking Water", who.int.
- [5] Danyuo Yiporo, Emmanuel K. Arthur, Salifu T. Azeko, John D. Obayemi, Ivy Mawusi Asuo, 2014. Design of Locally Produced Activated Carbon Filter from Agricultural Waste for Water Purification, *International Journal of Engineering Research & Technology (IJERT)* Vol. 3(6) (2014), pp1523-1534.
- [6] Khalifa, M. and Bidaisee, S., 2018, "The Importance of Clean Water", *Scholar Journal of Applied Sciences and Research*, 1(7), pp.17-20
- [7] Monney, I. and Antwi-Agyei, P., 2018, "Beyond the MDG water target to universal water coverage in Ghana: the key transformative shifts required". *Journal of Water, Sanitation and Hygiene for Development*, 8(2), pp.127-141. Doi: 10.2166/washdev.2018.176

- [8] Akpabio, E. and Takara, K., 2014, “Understanding and Confronting Cultural Complexities Characterizing Water, Sanitation and Hygiene (WASH) in sub-Saharan Africa”, *Water International*, 39(7). Doi: <http://dx.doi.org/10.1080/02508060.2015.981782>
- [9] Salaam-Blyther, T., 2012, “Global Access to Clean Drinking Water and Sanitation: U.S. and International Programs”, Congressional Research Service.
- [10] LENNTECH, "Water Treatment solutions," [Accessed on 2<sup>nd</sup> Oct. 2021]. <https://www.lenntech.com/processes/heavy/heavy-metals/heavy-metals.htm>.
- [11] CSIR, "Pollution of Ghana’s water bodies: CSIR predicts water crisis in 2030," Council for scientific and industrial research (2016). [Accessed 2021]. <https://www.csir.org.gh/index.php/multimedia/news/item/414-pollution-of-ghana-s-water-bodies-csir-predicts-water-crisis-in-2030>.
- [12] C. D. C. (Center for Disease Control and Prevention) “Progress Toward Global Eradication of Dracunculiasis”. *Morbidity and Mortality Weekly Report (MMWR)* Vol.57, 2008, pp1173-1176.
- [13] Eberhard, R., 2019, “Access to Water and Sanitation in Sub-Saharan Africa”. Part I- Synthesis Report, Eschborn, Germany, Deutsche Gesellschaft für Internationale Zusammenarbeit (GIZ) GmbH, pp.1-88.
- [14] M. Thompson, "A critical review of water purification technology appropriate for developing countries: Northern Ghana as a case study," *Desalination and Water Treatment*, Vol. 54(13) (2014) pp. 3487–3493.
- [15] Tchounwou, P. B., Yedjou, C. G., Patlolla, A. K. and Sutton, D. J. Heavy Metals Toxicity, and the Environment. *EXS*, Volume 101, (2012) pp 133-135.

- [16] K. Ofosu-Budu and D. B. Sarpong, "Oil Palm industry in Africa: A value chain and smallholders' study in Ghana," in *Rebuilding West Africa's Food Potential*, 2013, pp. 349-388
- [17] A. Eye, "Coconut tipped to be next big export commodity in Ghana after cocoa," Joy Online, 6 April 2021. [Online]. Available: <https://www.myjoyonline.com/coconut-tipped-to-be-next-big-export-commodity-in-ghana-after-cocoa-african-eye-report/>. [Accessed 1 January 2021]
- [18] S. Thangamalathi and V. Anuradha, "Role of Inorganic Pollutants in Freshwater Ecosystem - A Review", *International Journal of Advanced Research in Biological Science*, vol. 5(11)(2018) pp. 39-49.
- [19] WHO, "Guidelines for Drinkingwater Quality," vol. 1(3)(2017).
- [20] L. K. S. Lartey, "Design of a water filtration system for particulate absorption, heavy metal removal and water quality analysis", 2021.
- [21] Abida Begum, Harikrishna S., Irfanullah Khan. *International Journal of Chem Tech Research*. Vol .1(2) (2009) pp245-249.
- [22] Sher Ali Khan, Zahoor Ud Din, Ihsanullah, and Ahmad Zubair. *I.J.S.N.*, Vol.2(3) (2011) pp648-652.
- [23] Mohod C. V., Dhote J., Review of heavy metals in drinking water and their effect on human health. *International Journal of Innovative Research in Science, Engineering and Technology*. Volume 2(7), (2013), pp 2993-2996.
- [24] N. Akhtar, M. I. S. Ishak, S. A. Bhawani and K. Umar, "Various Natural and Anthropogenic Factors Responsible for Water Quality Degradation: A Review," *Water*, vol. 13 (2660) (2021), pp. 1-35.

- [25] Edwards B. History of Water Filtration (2016). Retrieved on 16<sup>th</sup> Nov. 2021.  
<https://haguewaterofmd.com/history-water-filtration/>
- [26] Hilal, N. and J. Wright, C., 2018, "Exploring the Current State of Play for Cost-effective Water Treatment by Membranes", *npj Clean Water*, 1(8). Doi: <https://doi.org/10.1038/s41545-018-0008-8>
- [27] Thompson, T., Sobsey, M. and Bartram, J., 2003, "Providing Clean Water, Keeping Water Clean: An Integrated Approach". *International Journal of Environmental Health Research*, 13(1), pp.89-94.
- [28] Mintz, E., Bartram, J., Lochery, P. and Wegelin, M., 2001," Not Just a Drop in the Bucket: Expanding Access to Point-of-Use Water Treatment Systems". *American Journal of Public Health*, 91(10), pp.1565-1570
- [29] S. L. Prabu and S. Timmakondu, "Extraction of Drug from the Biological Matrix: A Review," *Applied Biological Engineering- Principles and Practices(2012)* , pp. 379-506
- [30] T. R. Miller, "Optimizing Performance of Ceramic Pot Filters in Northern Ghana and Modeling Flow through Paraboloid-Shaped Filters", 2011.
- [31] Schiffler M. Perspectives and challenges for desalination in the 21st century. *Desalination* Volume 165, (2004), pp 1-9.
- [32] "Puretec Industrial Water | What is Reverse Osmosis?", Puretecwater.com [Online]. Available: <https://puretecwater.com/reverse-osmosis/what-is-reverse-osmosis>. [Accessed: 22-Dec- 2021].

- [33] DeSilva F. J., Exploring the Multifunctional nature of activated carbon filtration. Water Quality Products. (2000).
- [34] Bansal, R. C., & Goyal, M. (2005). *Activated carbon adsorption*. CRC press.
- [35] E. Annan, "Clay Ceramic Materials for Water Filtration: Properties, Processing and Performance," Abuja , 2016.
- [36] Dies, R., 2003, *Development of a Ceramic Water Filter for Nepal*, Master's thesis, Department of Civil and Environmental Engineering, Massachusetts Institute of Technology.
- [37] Gundry, S., Wright, J. and Conroy, R., 2004. "A Systematic Review of the Health Outcomes Related to Household water quality in developing countries". *Journal of Water and Health*, 2(1), pp.1-13.
- [38] Obi, C. and George, P., 2011. "The Microbiological and Physico-Chemical Analysis of Borehole Waters used by Off-Campus Students of Michael Okpara University of Agriculture, Umudike (MOUUAU), Abia State, Nigeria". *Research Journal of Biological Sciences*, 6(11), pp.602-607.
- [39] Henry, M., Maley, S. and Mehta, K., 2013. "Designing a Low-Cost Ceramic Water Filter Press". *International Journal for Service Learning in Engineering*, 8(1), pp.62-77.
- [40] Nair, C. and MophinKani, K., 2017. "Effectiveness of Locally Made Ceramic Water Filters for Household Water Purification". *International Journal of Emerging Technology and Advanced Engineering*, 7(1).
- [41] Soppe, A., Heijman, S., Gensburger, I., Shantz, A., van Halem, D., Kroesbergen, J., Wubbels, G. and Smeets, P., 2014. "Critical Parameters in the Production of Ceramic Pot Filters for

Household Water Treatment in Developing Countries". *Journal of Water and Health*, 13(2), pp.587-599.

[42] Victor A., Ribeiro J., Araujo F.S., Study of PDMS characterization and its applications in biomedicine: A review, *Journal of Mechanical Engineering and Biomechanics*, Volume 4, (2019), Issue 1, pp 1-9

[43] Hemmilä S, Cauch-Rodríguez J.V., Kreutzer J, Kallio P., Rapid, simple, and cost-effective treatments to achieve long-term hydrophilic PDMS surfaces. *Applied Surface Science*. Volume 24, (2012), pp 9864-9875.

[44] Zhao J., Sheadel D. A., Xue W., Surface treatment of polymers for the fabrication of all-polymer MEMS devices. *Sensors and Actuators A: Physical*; Volume 187, (2012), pp 43-49.

[45] Kuncova-Kallio J., Kallio P. J., PDMS and its suitability for analytical microfluidic devices. In *Engineering in Medicine and Biology Society. 28th Annual International Conference of the IEEE*. (2006), pp. 2486-2489.

[46] Martin S., Bhushan B. Transparent, wear-resistant, super hydrophobic and superoleophobic poly (dimethylsiloxane) (PDMS) surfaces. *Journal of colloid and interface science*. Volume 488, (2017), pp 118-26.

[47] S. Mustapha, T. J. Oladejo and N. M. Muhammed, "Fabrication of porous ceramic pot filters for adsorptive removal of pollutants in tannery wastewater," *Scientific African* , vol. 11 (2021).

[48] E. A. Zereffa and T. Desalegn, "Preparation and characteristics of sintered clay ceramic membranes water filters," *Open Material Science*, vol. 5(2019) pp. 24-33.

- [49] W. Zhong, X. Ji, C. Li, J. Fang and F. Liu, "Determination of Permeability and Inertial Coefficients of Sintered Metal Porous Media Using an Isothermal Chamber," *Applied Sciences*, vol. 8 (2018) pp. 1-17.
- [50] LENNTECH, "Turbidity," LENNTECH , 2021. [Online]. Available: <https://www.lenntech.com/turbidity.htm#What%20is%20turbidity?>. [Accessed on 10<sup>th</sup> Jan. 2022]
- [51] E. Annan, "Clay Ceramic Materials for Water Filtration: Properties, Processing and Performance," Abuja , 2016.
- [52] Keane TJ, Badylak SF. Biomaterials for tissue engineering applications. In *Seminars in pediatric surgery* 2014 Jun 1 (Vol. 23, No. 3, pp. 112-118)
- [53] Dullien, F. (1979), *Porous Media, Fluid Transport and Pore Structure*, Elsevier, New York.
- [54] D. S. Lantagne, "Investigation of the Potters for Peace Colloidal Silver Impregnated Ceramic Filter," USAID , Seattle, 2001.
- [55] D. v. Halem, H. v. d. Laan, A. Soppe and S. Heijman, "High Flow ceramic pot filters," *Water Research*, vol. 124(2017) pp. 398-406.
- [56] J. Brown and M. Sobsey, "Microbiological effectiveness of locally produced ceramic filters for drinking water treatment in Cambodia," *Journal of Water and Health*, vol. 8(1)(2020) pp. 1-10.
- [57] WHO, "Evaluating household water treatment options: health-based targets and microbiological performance specifications.," NMI. Classif WA , 2011.



- [58] D. v. Halem, J. C. v. Dijk, G. Amy and S. G. J. Heijman, "Ceramic silver-impregnated pot filters for household drinking water treatment in developing countries: Material characterization and performance study," *Water Science & Technology Water Supply*, 2007.
- [59] A. J. A, "Rule of Mixture fro Composites". [Online]. Available: <https://crescent.education/wp-content/uploads/2021/03/Rule-of-Mixture-of-composites.pdf> [Accessed on 4<sup>th</sup> Feb. 2022]
- [60] Schneider F., Fellner T., Wilde J., Wallrabe U., Mechanical Properties of Silicones for MEMS. *Journal of Micromechanics and Microengineering*. (2008), pp 1-9.
- [61] S. E. Günaslan, A. Karaşin and M. E. Öncü, "Properties of FRP Materials for Strengthening," *International Journal of Innovative Science, Engineering & Technology*, vol. 1(9)(2014) pp. 656-660.
- [62] E. Chiaha, "Different types of water pump and their application," *GZ Industrial Supplies* , 20 January 2021. [Online]. Available: <https://www.gz-supplies.com/news/different-types-of-water-pump-and-their-application/>. [Accessed on 28<sup>th</sup> Dec. 2021].
- [63] Plappaly, A., Chen, H., Ayinde, W., Alayande, S., Usuro, A., Friedman, K., Dare, E., Ogunyale, T., Yakub, I., Leftwich, M., Malatesta, K., Rivera, R., Brown, L., Soboyejo, A. and Soboyejo, W., 2011. "A Field Study on the Use of Clay Ceramic Water Filters and Influences on the General Health in Nigeria". *Journal of Health Behaviour and Public Health*, 1(1), pp.1-14.
- [64] Grema, A. S., Idriss, I. M., Alkali, A.N., Ahmed, M. M. and Iyodo, H. M., 2021. "Production of Clay-based Ceramic Filter for Water Purification". *European Journal of Engineering and Technology Research*, 6(7), pp. 140-143. Doi: <http://dx.doi.org/10.24018/ejers.2021.6.7.2623>

- [65] The Ceramics Manufacturing Working Group, *Best Practice Recommendations for Local Manufacturing of Ceramic Pot Filters for Household Water Treatment*, 2011, Ed. 1. Atlanta, GA, USA: CDC.
- [66] M. Chaudhuri and S. N. B. Saminal, "Coconut coir activated carbon: an adsorbent for removal of lead from aqueous solution," *Ravage of the Planet III*, vol. 148 (2011) pp. 95-104.
- [67] C. Matthews, "Mechanical seals-improving design reliability," ScienceDirect, 1998. [Online]. Available: <https://www.sciencedirect.com/topics/engineering/stress-raiser>. [Accessed on 2<sup>nd</sup> Feb. 2022].
- [68] GAA, "Galvanizers Association of Australia," 2020. [Online]. Available: <https://gaa.com.au/welding/#:~:text=Galvanized%20steels%20are%20welded%20easily,are%20simple%20and%20well%20established..> [Accessed on 25<sup>th</sup> Jan. 2022].
- [69] Shrivastava, A., 2018. *Plastic Properties and Testing*.
- [70] Chakraborty, B. and Ratna, D., 2020. *Polymers for Vibration Damping Applications*.
- [71] Prajapati, D. and Mishra, A., 2021. Compressive strength. *Reference Module in Materials Science and Materials Engineering*.
- [72] Rice, R.W., 1971. The compressive strength of ceramics. In *Ceramics in Severe Environments* (pp.195-229).Springer,Boston,MA.
- [73] Richerson, D., Richerson, D. and Lee, W., 2022. *Mordern Ceramic Engineering: Properties, Processing, and Use in Design*. 3rd ed. New York: Taylor and Francis Group, pp.221-223.
- [74] Shukur, M., Aswad, M. and Bader, S., 2018. Effects of sawdust and rice husk additives on physical properties of ceramic filter. *Journal of University of Babylon*, 26(1).

[75] Heidari, A. and Tavakoli, D. (2013). A study of the mechanical properties of ground ceramic powder concrete incorporating nano-SiO<sub>2</sub> particles, *Construction and Building Materials*, 38, pp. 255-264.

[76] Durgun, M. Y., Atahan, H. N. (2018). Strength, elastic and microstructural properties of SCCs' with colloidal nano silica addition, *Construction and Building Materials*, 158, pp. 295-307.

[77] Faraj, R.H., Mohammed, A.A. and Omer, K.M. (2022). Self-compacting concrete composites modified with nanoparticles: A comprehensive review, analysis and modeling, *Journal of Building Engineering*, 50.

## Appendices

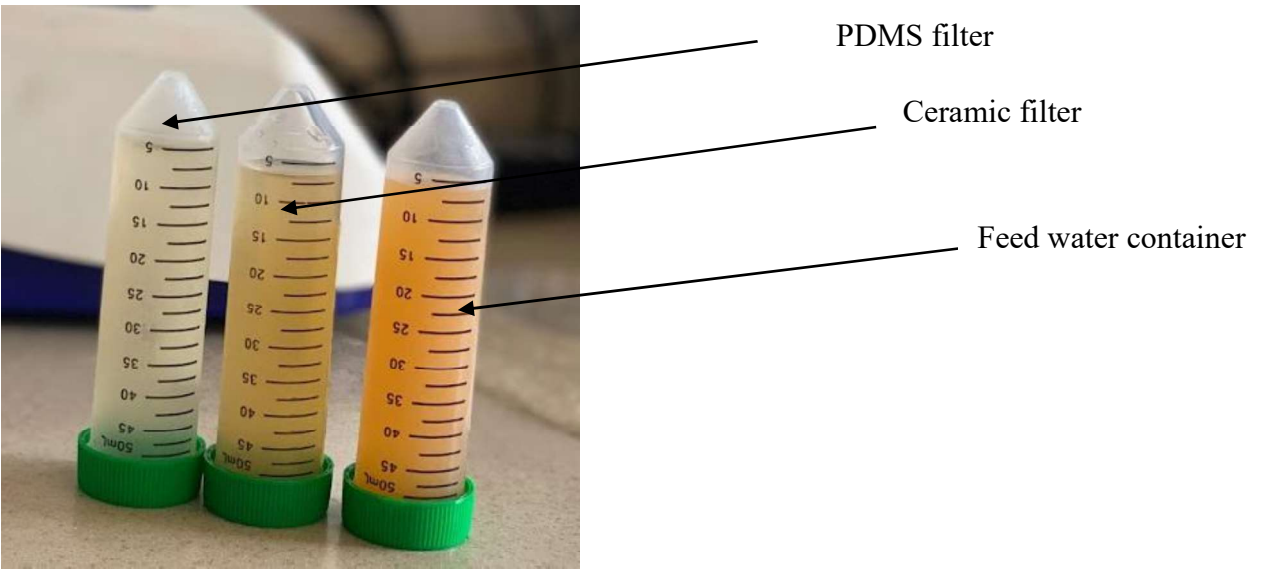
### Appendix A: Water Analysis Tests



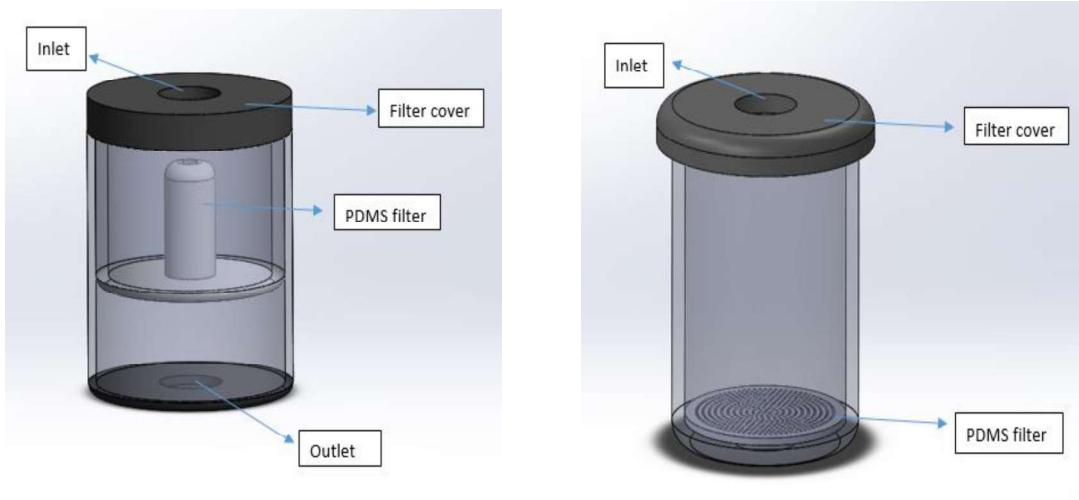
**A1:** Experimental setup for control test using commercial activated carbon



**A2:** Water samples from river Densu, nana mall river and Abandza river at Akwatia.

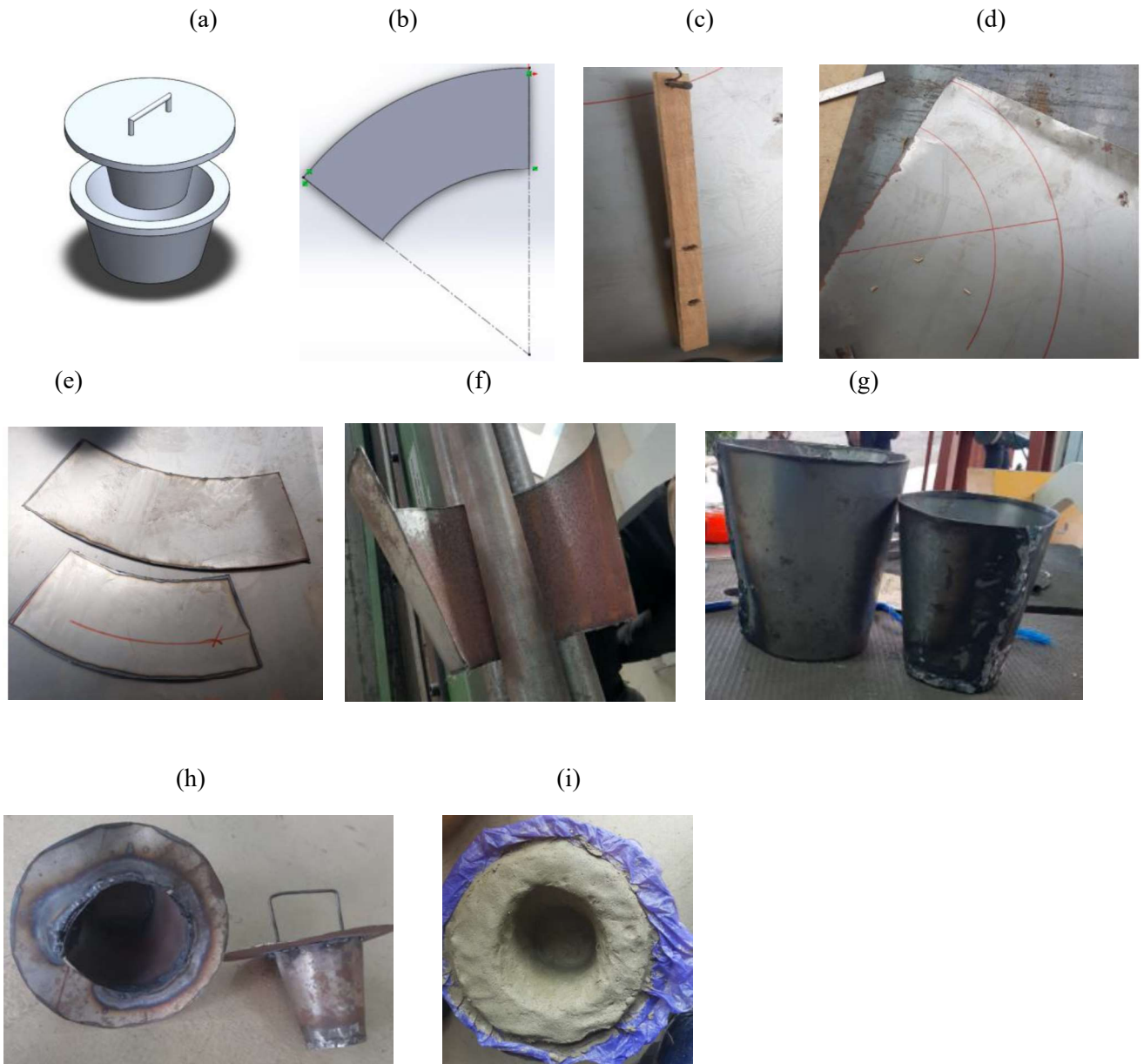


**A3:** Nana Mall River before and after filtration.



**A4:** Two other designs that were considered for the PDMS filter.

**Appendix B: Procedure for making Male and Female Mould for Ceramic Water Filter and for determining Density and Porosity**



a) exploded view of male and female mold    b) cone development in SolidWorks    c) marking and drilling of plywood for drawing our arcs    d) arcs marked out with 45 degree line marked from the centre    e) cut-out inner and outer cones    f) rolling the cut out shapes into a conical shape    g) welding and finishing of welded surfaces    h) completed male and female mold    i) soft-worked clay paste molded into the required shape

## **B1: Procedure for making male and female mold**

The male and female mold was used to get the shape of the ceramic water filter. It was made with 1mm steel that was cut, rolled and welded. The following are the steps to make the mold:

- i. The cone development for the male and female molds were developed in SolidWorks 2021 . This was done to obtain the arc dimensions to be cut from the steel.
- ii. The inner cone(male) had a height of 12 cm. The base diameter was 6.5 cm while the upper diameter was 10 cm. the outer arc radius was 41.5 cm and the inner arc radius was 29.4 cm.
- iii. The outer cone(female) had a base diameter of 8.5 cm and an upper diameter of 12cm. the height was 14 cm. the outer arc radius was 48.26 cm and the inner arc radius was 34.26 cm.
- iv. The arc radii were marked on a long plywood strip. A common centre mark was used to obtain all for arc radii(two for male and two for female mold). Holes were drilled at the marks to the size of a board marker.
- v. A dot punch was used to locate an appropriate centre of the 1mm steel slab while the arc lengths were drawn with the help of the marker and the holes.
- vi. A 45-degree line was drawn from the centre (marked by the dot punch) to cut the arcs.
- vii. The arcs were cut out with an angle grinder
- viii. The edges were smoothed with a bench grinder
- ix. The shapes were bent into a cone shape with the steel slip roll

The shapes were welded into the form of the cone. The male mold was filled with rocks and sand to make it heavy. A cover and a handle were welded on top for easy use.

## B2: Procedure for determining porosity and density

The density and the porosity of the different clay-sawdust rectangular samples were determined together because similar parameters are required for each characteristic. The following steps were used:

- i. Five samples were selected from each clay-sawdust ratio. The mass of each sample was measured and recorded. Microsoft excel was used for this activity.
- ii. The length, breadth and thickness of each sample were recorded, and the bulk volume computed.
- iii. The samples were labelled and left in 500ml of water overnight.
- iv. The next day, the samples were removed from the water and the water drops wiped from the surface. The samples were weighed again and the saturated mass recorded.
- v. The weight of water is calculated as saturated mass - dry mass. The weight of water represents the weight of fluid that occupies the pores in the samples .

Dividing the weight of water by the density of water gives the volume occupied by the pores.

$$\text{(Volume of pores = } \frac{\text{weight of water}}{1\text{g/cm}^3} \text{ )}$$

- vi. Subtracting volume of pores from bulk volume gives the true volume of the sample.

$$\text{(True volume = bulk volume – volume of pores)}$$

- vii. Porosity =  $\frac{\text{Volume of pores}}{\text{bulk volume}}$  and Density =  $\frac{\text{dry mass}}{\text{True volume}}$



## Appendix C: Pump Sizing Calculations

$$H_{total} = H_s + H_D + (P_{RT} - P_{RES})$$

where  $H_s$  = Static head (m),  $H_D$  = Dynamic head (m),

$P_{RT}$  = Pressure on the surface of the water in the receiving tank and

$P_{RES}$  = Pressure on the surface of the water

Assuming equal pressure results in the expression:

$$H_{total} = H_s + H_D$$

The head due to friction within the system is expressed as:

$$H_D = \frac{Kv^2}{2g}$$

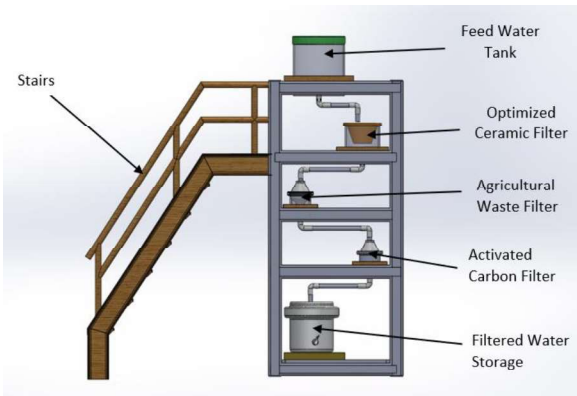
where K is the loss coefficient, v is the velocity of the pipe (m/s), and g is the acceleration due to gravity.

The loss coefficient constitutes the coefficient associated with the fittings ( $K_f$ ) used in the pipework of the system to pump the water from the surface of its source to that of the receiving tank and the friction coefficient ( $K_{pipe}$ ) associated with the pipes within the system. Hence, mathematically, the loss coefficient can be expressed as:

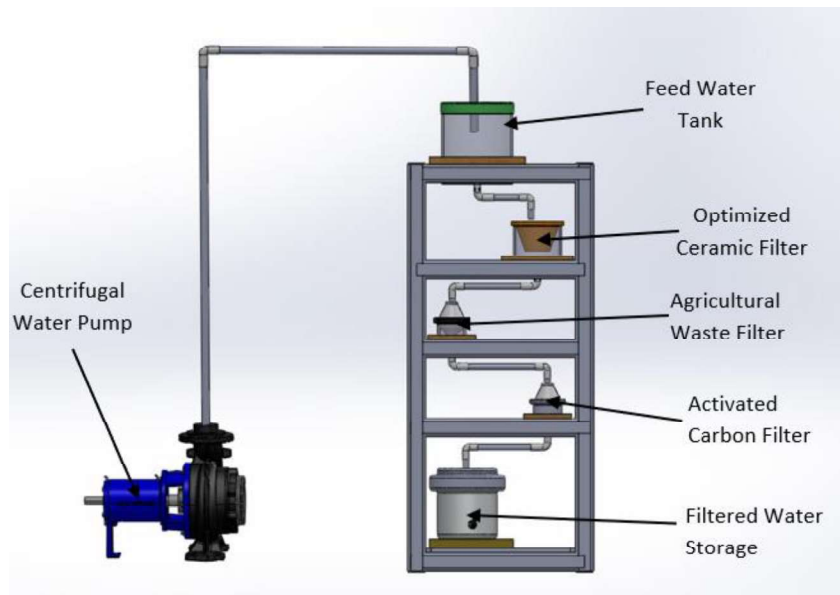
$K = K_f + K_{pipe}$  where  $K_{pipe} = \frac{fL}{D}$  where f is the friction coefficient and L is the length of the pipe. The friction coefficient is determined by the Colebrook White equation given by:

$$f = \frac{0.25}{\left[ \log \left\{ \frac{k}{3.7D} + \frac{5.74}{Re^{0.9}} \right\} \right]^2}$$

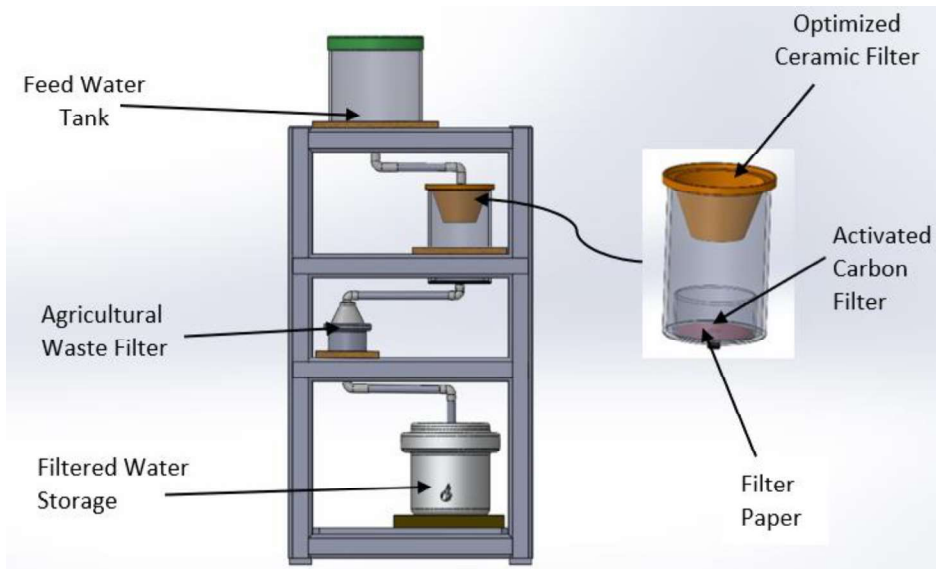
## Appendix D: Proposed Designs



### D1: Conceptual Design 1

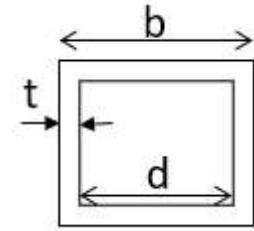
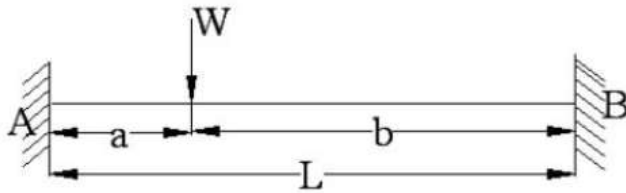


### D2: Conceptual Design 2



**D3:** Conceptual Design 3

## Appendix E: Steel Structure Analytical Calculations



Where  $L = 650\text{mm}$ ,  $a = 212\text{mm}$ ,  $b = 438\text{mm}$  and  $W = 662.12\text{N}$

### Load Analysis:

$$M_A = \frac{-Wb^2a}{L^2} = 63.73\text{KN}\cdot\text{mm}$$

$$M_B = \frac{-Wa^2b}{L^2} = 30.85\text{KN}\cdot\text{mm}$$

$R_A$  and  $R_B$  were determined

The Shear Force and Bending Moment diagram suggested that the critical location is at C

### Stress Analysis:

Type: Bending, critical location is at C

$$M_{max} = M_C = \frac{M}{Z}$$

$$\sigma_{max} = \frac{M}{Z}, \text{ where } Z = \frac{I}{c}, c = \frac{b}{2}$$

$$I = \frac{1}{12}bh^3 - \frac{1}{12}[(b - 2t) \times (b - 2t)^3]$$

Uniaxial stress element results in  $\sigma_1 = \sigma_{max}$

### Material:

Given: Galvanized steel  $S_y = 300\text{MPa}$

$$\sigma_1 = \tau_{max}$$

Using Von Misses theory:

$$n = \frac{0.577S_y}{\tau_{max}}, \text{ assuming a factor of safety of 2}$$

$$86.55 [b^4 - (b - 2t)^4] = 842.214 \times 10^3 b$$

Assuming a thickness of 10mm results in a b value of 119.35mm

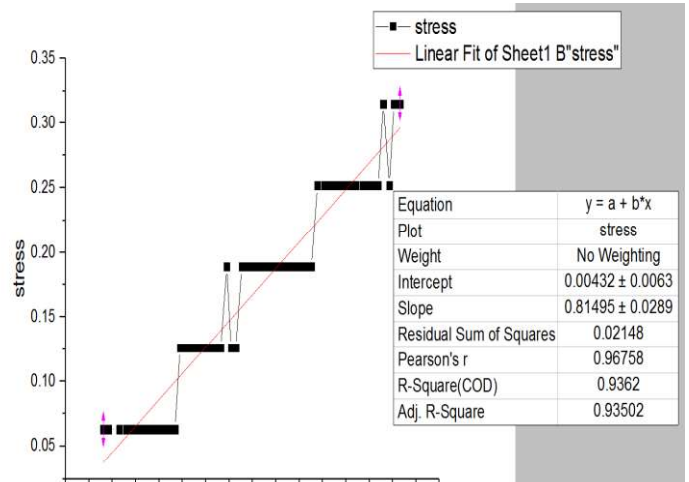
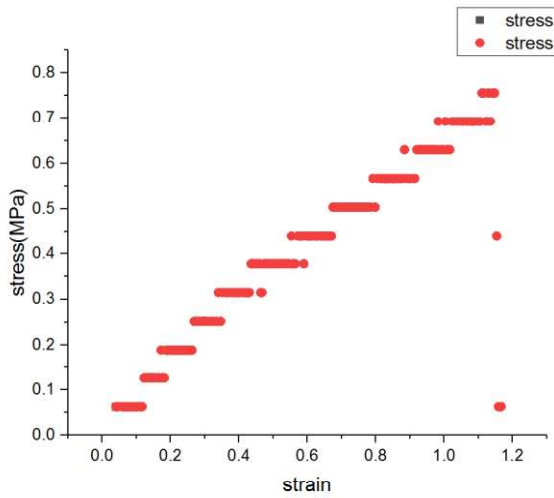
Using the standard table, a thickness of 10mm corresponds to a size  $b \times b$  to be  $120 \times 120$

## Appendix F: Fabrication



**F1:** Dogbone mould for the tensile strength testing of PDMS samples.

## Appendix G: Stress stain graphs obtained from Origin



**G1:** Stress strain graph and the linear fit of the linear part of the curve with the slope representing the Young's Modulus for PDMS sample.

## Appendix H: Water quality analysis equipment

(a)



(b)



(c)



(d)



**H1:** (a) pH sensor (b) turbidity sensor (c) Conductivity sensor (d) temperature probe

## Appendix I: Statistical analysis for PDMS membrane

Normality Test (27-Apr-22 11:46:28)

Notes

Input Data

Descriptive Statistics

NormalityTest

Shapiro-Wilk

	DF	Statistic	p-value	Decision at level(5%)
10:1	4	0.87638	0.32342	Can't reject normality
5:1	4	0.87371	0.31246	Can't reject normality

10:1: At the 0.05 level, the data was significantly drawn from a normally distributed population.  
 5:1: At the 0.05 level, the data was significantly drawn from a normally distributed population.

**t-Test: Two-Sample Assuming Unequal Variances**

	<i>ten to one</i>	<i>five to one</i>
Mean	0.7765025	0.47074
Variance	0.003276278	0.004188141
Observations	4	4
Hypothesized Mean Difference	0	
df	6	
t Stat	7.078091806	
P(T<=t) one-tail	0.00019936	
t Critical one-tail	1.943180281	
P(T<=t) two-tail	0.00039872	
t Critical two-tail	2.446911851	

**I1** : Normality tests and independent t-test for unequal variance.



## Appendix J: FTIR and XRF: Laboratory test and Analysis

**Table J1: FTIR:** Absorbance band and functional groups identified for Birsana and Nyennol

Absorbance bands in Birsana Wavenumbers $\text{cm}^{-1}$	Matching Functional group	Absorbance bands in Nyennyol Wavenumbers $\text{cm}^{-1}$	Matching Functional group
3365.00	Normal “polymeric” OH stretch	3272.42	Hydroxyl group, H-bonded OH stretch
2917.01	Methyne C-H stretch	2917.50	Methyne C-H stretch
2843.23	Methoxyl, methyl ether O-CH <sub>3</sub> , C-H stretch	1606.58	Carboxylate(carboxylic acid salt)
1604.70	Carboxylate(carboxylic acid salt)	1444.44	Inorganic ion (carbonate ion)
1513.70	C=C-C Aromatic ring stretch	1315.01	Inorganic ion (nitrate ion)
1443.70	Carbonate ion	1205.97	Alcohol and hydroxy compound(Phenol, C-O stretch)
1367.44	Nitrate ion	1029.41	Ether and Oxy compound(aromatic ethers, aryl-O stretch)
1321.64	Dialkyl/aryl sulfones	777.69	Aliphatic chloro compounds(C-Cl) stretch
1238.31	Methyne(skeletal C-C vibrations)	512.11	Aliphatic iodo compounds, C-I stretch
1031.15	Methylene (skeletal C-C vibrations)	425.25	-fingerprint region
411.00	-fingerprint region		

**Table J2:** XRF analysis of Birsana, identified elements and oxides

Elements	Mass(%)	Oxides	Mass (%)
Magnesium(Mg)	2.26	Magnesium Oxide (MgO)	13.2
Aluminium(Al)	0.537	Aluminium Oxide (Al <sub>2</sub> O <sub>3</sub> )	4.44
Silicon(Si)	4.05	Silicon Oxide (SiO <sub>2</sub> )	41.3
Phosphorus(P)	0.171	Phosphorus Pentoxide(P <sub>2</sub> O <sub>5</sub> )	1.85
Sulphur(S)	0.069	Sulphur Trioxide (SO <sub>3</sub> )	1.11
Chlorine(Cl)	0.333		
Potassium(K)	1.5	Potassium Oxide(K <sub>2</sub> O)	12.6
Calcium(Ca)	1.42	Calcium Oxide (CaO)	18.6
Titanium(Ti)	0.0406	Titanium Dioxide (TiO <sub>2</sub> )	0.866
Vanadium(V)	0.0016	Vanadium Oxide(V <sub>2</sub> O <sub>5</sub> )	0.0531
Chromium(Cr)	0.0046	Chromium (III) Oxide (Cr <sub>2</sub> O <sub>3</sub> )	0.0865
Manganese(Mn)	0.0274	Manganese Oxide (MnO)	0.461
Iron (Fe)	0.222	Ferric Oxide(Fe <sub>2</sub> O <sub>3</sub> )	4.24
Cobalt (Co)	0.0007	Cobalt (III) Oxide	0.0244
Nickel(Ni)	0.0011	Nickel Oxide (NiO)	0.0214
Zinc (Zn)	0.0026	Copper Oxide (CuO)	0.0483
Copper (Cu)	0.0028	Zinc Oxide (ZnO)	0.0499

Gallium (Ga)	0.0001	Arsenic Trioxide( $\text{As}_2\text{O}_3$ )	0.0008
Bromine(Br)	0.0002		
Rubidium (Rb)	0.0006	Rubidium Oxide ( $\text{Rb}_2\text{O}$ )	0.0098
Strontium (Sr)	0.0071	Strontium Oxide ( $\text{SrO}$ )	0.131
Tin(Sn)	0.0004	Tin (IV) Oxide( $\text{SnO}_2$ )	0.0046
Barium(Ba)	0.0052		
Hafnium(Hf)	0.0005	Hafnium (IV) Oxide ( $\text{HfO}_2$ )	0.0114
Tantalum (Ta)	0.0005	Tantalum Pentoxide ( $\text{Ta}_2\text{O}_5$ )	0.0125
Gold(Au)	0.0002	Gold Oxide ( $\text{Au}_2\text{O}$ )	0.003
Lead(Pb)	0.0004	Lead Oxide ( $\text{PbO}$ )	0.005
Zirconium (Zr)	0.0505	Zirconium Oxide ( $\text{ZrO}_2$ )	0.974
Oxygen(O)	89.3	Uranium Octoxide( $\text{U}_3\text{O}_8$ )	0.0047

**Table J3:** XRF analysis of Nyennyol, identified elements and oxides

Elements	Mass (%)	Oxides	Mass (%)
Magnesium (Mg)	0.81	Magnesium Oxide (MgO)	2.22
Aluminium (Al)	0.403	Aluminium Oxide (Al <sub>2</sub> O <sub>3</sub> )	2.52
Silicon (Si)	2.6	Silicon Oxide (SiO <sub>2</sub> )	21.4
Phosphorus(P)	0.124	Phosphorus Pentoxide(P <sub>2</sub> O <sub>5</sub> )	0.482
Sulphur(S)	0.06	Sulphur Trioxide (SO <sub>3</sub> )	0.677
Chlorine (Cl)	0.274		
Potassium(K)	0.462	Potassium Oxide(K <sub>2</sub> O)	2.96
Calcium (Ca)	6.29	Calcium Oxide (CaO)	63.1
Titanium (Ti)	0.0404	Titanium Dioxide (TiO <sub>2</sub> )	0.848
Vanadium(V)	0.0015	Vanadium Oxide(V <sub>2</sub> O <sub>5</sub> )	0.0429
Chromium (Cr)	0.0023	Chromium (III) Oxide (Cr <sub>2</sub> O <sub>3</sub> )	0.0473
Manganese (Mn)	0.0145	Manganese Oxide (MnO)	0.283
Iron (Fe)	0.146	Ferric Oxide (Fe <sub>2</sub> O <sub>3</sub> )	3
Nickel (Ni)	0.001	Cobalt (III) Oxide (Co <sub>2</sub> O <sub>3</sub> )	0.0094
Zinc (Zn)	0.0021	Nickel Oxide (NiO)	0.0191
Copper (Cu)	0.0012	Copper Oxide (CuO)	0.0441
Bromine (Br)	0.0002	Zinc Oxide (ZnO)	0.0245

Rubidium (Rb)	0.0008	Arsenic Trioxide (As <sub>2</sub> O <sub>3</sub> )	0.0002
Strontium (Sr)	0.037	Selenium Oxide (SeO <sub>2</sub> )	0.0018
Tin (Sn)	0.0005	Rubidium Oxide (Rb <sub>2</sub> O)	0.0124
Barium (Ba)	0.0046	Strontium Oxide (SrO)	0.68
Hafnium (Hf)	0.0004	Tin (IV) Oxide (SnO <sub>2</sub> )	0.0067
Tantalum (Ta)	0.0008	Barium Oxide (BaO)	0.0471
Gold (Au)	0.0002	Hafnium (IV) Oxide (HfO <sub>2</sub> )	0.0103
Iridium (Ir)	0.0002	Tantalum Pentoxide (Ta <sub>2</sub> O <sub>5</sub> )	0.013
Lead (Pb)	0.0005	Uranium Octoxide(U <sub>3</sub> O <sub>8</sub> )	0.0119
Zirconium (Zr)	0.0724	Lead Oxide (PbO)	0.0065
Oxygen(O)	88.7	Zirconium Oxide (ZrO <sub>2</sub> )	1.43

## Appendix K: Properties of Clay-Sawdust Samples and Water Quality Analysis

**Table K1:** A table showing the apparent porosity and density values of the different clay-sawdust ratios.

Clay-Sawdust Ratio	Apparent Porosity (%)	Density ( $\text{gcm}^{-3}$ )
100-0	29.0223	2.6443
60-40	32.1764	2.0096
55-45	34.9000	2.0233
50-50	33.4062	1.9945
45-55	40.1827	2.0901

(a)



(b)



**Figure K1:** a) magnified image of 100-0 clay-sawdust ratio surface b) magnified image of 55-45 clay-sawdust ratio surface.

**Table K2:** Turbidity, conductivity, and pH of water samples from all five filters.

	Conductivity ( $\mu\text{S}/\text{cm}$ )	pH	Turbidity (NTU)
WHO standard	Less than 400	6.5-8.5	Less than 5
Initial results	260.6026	6.8672	670

Clay-sawdust ratios	Conductivity ( $\mu\text{S}/\text{cm}$ )	PH	Turbidity (NTU)
100-0	237.5	6.34	91.5
60-40	261.1	5.28	48.4
55-45	252.2	4.91	10.7
50-50	258.4	5.30	33.4
45-55	254.1	5.33	8.9